

Perturbations and Causality in Gaussian Models

Armeen Taeb and Peter Bühlmann *

Seminar for Statistics, ETH Zürich

Abstract

Causal inference is understood to be a very challenging problem with observational data alone. Without making additional strong assumptions, it is only typically possible given access to data arising from perturbing the underlying system. To identify causal relations among a collections of covariates and a target or response variable, existing procedures rely on at least one of the following assumptions: i) the target variable remains unperturbed, ii) the hidden variables remain unperturbed, and iii) the hidden effects are dense. In this paper, we consider a perturbation model for interventional data (involving soft and hard interventions) over a collection of Gaussian variables that does not satisfy any of these conditions and can be viewed as a mixed-effects linear structural causal model. We propose a maximum-likelihood estimator – dubbed *DirectLikelihood* – that exploits system-wide invariances to uniquely identify the population causal structure from perturbation data. Our theoretical guarantees also carry over to settings where the variables are non-Gaussian but are generated according to a linear structural causal model. Further, we demonstrate that the population causal parameters are solutions to a worst-case risk with respect to distributional shifts from a certain perturbation class. We illustrate the utility of our perturbation model and the *DirectLikelihood* estimator on synthetic data as well as real data involving protein expressions.

1 Introduction

Identifying causal relations from observational data is challenging and often impossible. In the context of SCMs [24, 21], one possibility is to find the *Markov equivalence class* (MEC) of directed acyclic graphs under the faithfulness assumption [32] or the beta-min condition [31]. Some of the well-known algorithms for structure learning of MECs with observational data include the constraint based PC algorithm [29], score based greedy algorithm GES [5] and hybrid methods that integrate constraint based and score based methods such as ARGES [19]. In many applications though, we have available both observational and interventional or perturbation data, where the latter are coming from experiments with unknown targets. In genomics, for example, with the advance of gene editing technologies, high throughput interventional gene expression data is being produced [8]. Interventional data can be viewed as *perturbations* to components of the system and can offer substantial gain in identifiability: [12] demonstrated that combining interventional with observational data reduces ambiguity and enhances identifiability to a smaller equivalence class than the MEC, known as the I-MEC (Interventional MEC). A variety of methods have been proposed for causal structure learning from observational and interventional data. This includes the modified GES algorithm by [12] known as GIES, permutation-based causal structure learning [33], penalized maximum-likelihood procedure in Gaussian models [14], and methods based on causal invariance framework [17, 23]. For a more comprehensive list, see [9] and the references therein.

A common challenge for accurate structure learning is that there may be hidden variables for which it is expensive or impossible to obtain sample observations. Such unobserved variables pose a significant difficulty as the causal graphical model structure is not closed under marginalization; therefore, the graphical structure corresponding to the marginal distribution of the observed variables consists of potentially many confounding dependencies that are induced due to the marginalization over the hidden variables. There are causal structural learning methods that account for the presence of hidden variables. In the observational setting, two prominent examples are the Fast Causal Inference (and its variants) [29] for DAG learning and the two-stage deconfounding procedure [11] involving the sparse-plus-low rank decomposition framework [4] as the first stage and the standard DAG learning procedure in the second stage. As discussed earlier, the two-stage deconfounding procedure will only enable to

*Correspondence email: armeen.taeb@stat.math.ethz.ch

infer a certain MEC but not the causal parameter and structure itself. In the observational and interventional setting with unperturbed hidden variables and only shift interventions on the observed covariates, Causal Dantzig [25] consistently estimates the causal relations of a target variable assuming that the interventions do not directly affect the target variable. Such an assumption is relaxed in the backShift procedure [27] while it still requires that the hidden variables remain unperturbed for identifying the causal structure.

Guaranteed identifiability using these previous techniques for perturbation data relies on at least one of the following assumptions: i) the target variable remains unperturbed, ii) the hidden variables remain unperturbed, and iii) the hidden effects are dense. In this paper, we propose a modeling framework and an estimator that does not rely on any of these assumptions and yet identifies the population DAG structure. Fig 1 demonstrates a toy example of our setup among 4 observed variables X_1, X_2, X_3, X_4 and hidden variables H , and \mathcal{A} represents external variables (to the graphical structure among observed and hidden variables) that provide perturbations.

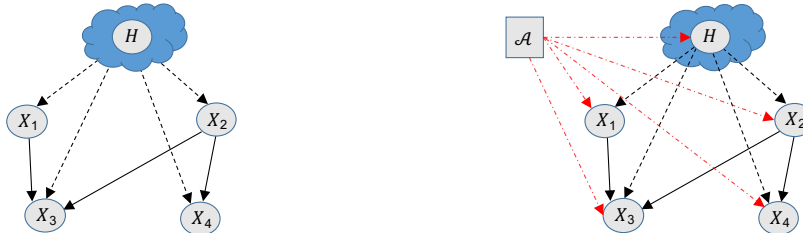


Figure 1: Toy example of 4 observed variables X_1, X_2, X_3, X_4 and hidden variables H where solid lines are connections among observed variables and dotted lines are connections between observed and hidden variables; left: without perturbations, right: perturbations \mathcal{A} on all components indicated with red dotted lines.

We consider a Gaussian structural causal model (SCM) specifying the perturbation model and the relationship between p observed variables $X \in \mathbb{R}^p$ and hidden variables $H \in \mathbb{R}^h$. We consider the setting with heterogeneous grouped data from different environments $e \in \mathcal{E}$. Here e denotes the index of an environment or a sub-population and \mathcal{E} is the space of different observed environments. As we will formalize in Section 2.1, each group or environment e corresponds to some perturbations of the underlying SCM. The grouped data, across different environments, is denoted by (X^e, H^e) with $e \in \mathcal{E}$. The SCM is parameterized by a connectivity matrix encoding the causal relationship among the observed variables, a coefficient matrix encoding the hidden variable effects, and nuisance parameters involving the noise variances and perturbation magnitudes among all of the variables. A key property of this modeling framework is that the connectivity matrix and the hidden variable coefficient matrix remain *invariant* across all of the perturbation environments. With this insight, we propose a maximum-likelihood estimator – dubbed *DirectLikelihood* – to score a given DAG structure. *DirectLikelihood* provides a flexible framework to incorporate additional knowledge including do-interventions when their intervention-locations are known or additional information on the perturbation structure (such as statistically identical perturbations on all of the observed variables). Further, the framework can be specialized to the setting considered by [25, 27] where the hidden variables are not perturbed across environments (i.e. \mathcal{A} does not point to H in Fig 1), or to the setting where there is no hidden confounding (i.e. H does not point to the covariates in Fig 1).

Besides the novel methodology, we provide conditions for which *DirectLikelihood* correctly identifies the population DAG structure. In particular, we demonstrate that with at least two interventional environments, where one of the environments consists of sufficiently large interventions on each of the observed variables, and the hidden effects satisfying a *hidden spuriousness* assumption, *DirectLikelihood* provides consistent estimates. The *hidden spuriousness* assumption for an environment e states that the hidden variables induce confounding dependencies among the observed variables; formally, there exists at least one pair of variables (X_k^e, X_l^e) such that $X_k^e \perp\!\!\!\perp X_l^e \mid \{X_{\setminus\{k,l\}}^e, H^e\}$ and $X_k^e \not\perp\!\!\!\perp X_l^e \mid X_{\setminus\{k,l\}}^e$, where $X_{\setminus\{k,l\}}^e$ denotes the collections of variables X^e excluding X_k^e, X_l^e . The *hidden spuriousness* assumption is substantially weaker than the hidden denseness assumption required in the two-stage deconfounding procedure in [11] which insists that there are many pairs of variables satisfying the condition above. Our theoretical results are further specialized to the setting where the hidden variables remain unperturbed across all of the environments or when there are no hidden variables. When the hidden variables are unperturbed, *DirectLikelihood* requires no assumption on the hidden structure for identifiability, whereas the two-stage deconfounding procedure still requires hidden denseness. We remark that the main focus of our analysis is on identifiability guarantees, and we discuss in Section 7 future work on understanding high-dimensional consistency properties of the *DirectLikelihood* procedure.

Further, we highlight a connection between distributional robustness and the causal parameters in our perturbation model. Specifically, we prove that the population causal parameters are solutions to a worst-case risk over the space of DAGs and distributional shifts from a certain perturbation class. Here, the risk is measured by the Kullback-Libeler divergence between the estimated and population Gaussian distributions. As with the DAG identifiability, the relation between causality and distributional robustness relies on the stringent assumption that the perturbations do not directly affect the target variable or the hidden variables [3, 26]. The results in this paper provided a more complete picture on the connection between perturbations, causality, and distributional robustness (see also Table 1).

As our final contribution, we propose an optimization procedure to solve *DirectLikelihood* and demonstrate the utility of our proposed estimator with synthetic data and real data involving protein expression data [28].

The outline of this paper is as follows. In Section 2, we describe the model for observational and perturbation data and its representation as a mixed-effects model, and then present the maximum-likelihood estimator *DirectLikelihood* to score a given DAG structure. In Section 3, we provide theoretical guarantees for the optimally scoring DAGs (scored via *DirectLikelihood*). In Section 4, the connection between the causal parameters of the proposed perturbation model and distributional robustness is explored. In Section 5, we present an optimization strategy for solving *DirectLikelihood* for a given DAG structure and how to use it to obtain the best scoring DAGs. In Section 6, we demonstrate the utility of our approach with real and synthetic data. We conclude with a discussion and future research directions in Section 7.

1.1 Related work

We have mentioned differences to backshift [27] and two-stage deconfounding procedures and provide more comparisons throughout the paper. *DirectLikelihood* is similar in spirit to approaches based on invariance principles [23, 25] as it exploits certain model parameters (such as the connectivity matrix and hidden variable effects) remaining unchanged across perturbations. However, a key difference between *DirectLikelihood* and these other techniques – in addition to being able to incorporate perturbations on the hidden variables – is that *DirectLikelihood* models the entire system of observed variables as opposed to just the regression of the target variable and the remaining observed variables. The virtue of this system-wide modeling is that all of the variables can experience perturbations without sacrificing consistency guarantees while the methods [23, 25] assume that the perturbations do not directly affect the target variable. This perspective was also adopted in the backShift procedure [27], although *DirectLikelihood* can allow for perturbations on the hidden variables. For a summary of the assumptions for *DirectLikelihood* as compared to competing methods, see Table 1.

Method	Perturbed target	Unperturbed hidden	Perturbed hidden
IV, ICP, Causal Dantzig	x	✓	x
two-stage deconfounding	✓	✓ hidden denseness	✓ hidden denseness
backShift	✓	✓	x
<i>DirectLikelihood</i>	✓	✓	✓ <i>hidden spuriousness</i>

Table 1: Comparison of *DirectLikelihood* with competing methods in the following settings: target variable is perturbed, hidden variables are unperturbed, and the hidden variables are perturbed. The methods are Instrumental Variables IV [1], Invariant Causal Prediction ICP [23], two-stage deconfounding [11] tailored for observational and interventional data, backShift [27] and our proposal *DirectLikelihood*.

1.2 Notation

We denote the identity matrix by \mathcal{I} , with the size being clear from context. The collection of positive-semidefinite matrices in \mathbb{S}^d is denoted by \mathbb{S}_+^d and the collection of strictly positive-definite matrices by \mathbb{S}_{++}^d . The collection of non-negative vectors in \mathbb{R}^d is denoted by \mathbb{R}_+^d and strictly positive vectors by \mathbb{R}_{++}^d . Given a matrix $M \in \mathbb{R}^{d \times d}$ and a set $S \subseteq \{1, 2, \dots, d\}$, we denote the restriction of M to rows and columns indexed by S by $[M]_S$. We denote the number of nonzeros in a matrix $M \in \mathbb{R}^{p \times p}$ by $\|M\|_{\ell_0}$. We apply a similar notation to count the number of edges in a graph. Given a DAG \mathcal{D} , we denote $\text{moral}(\mathcal{D})$ to be the moralization of \mathcal{D} . We denote the the index set

of the parents of a random variable X_p by $\text{PA}(p)$. We denote the index set for the descendants and ancestors by $\text{DES}(p)$ and $\text{ANC}(p)$, respectively. Further, letting \mathcal{D} be the DAG underlying a collection of variables (X, H) , we denote the subgraph of \mathcal{D} restricted to the variables X by \mathcal{D}_X and likewise for \mathcal{D}_H . Given a matrix $M \in \mathbb{R}^{d_1 \times d_2}$, we denote $\|M\|_2$ to be the largest singular value (spectral norm). For two vectors $z_1, z_2 \in \mathbb{R}^d$, we denote $z_1 \succeq z_2$ to denote element-wise inequality. Finally, for random variables V_1, V_2 and random vectors Z , we use the notation $\rho(V_1, V_2|Z)$ to denote the partial correlation between V_1 and V_2 given Z .

2 Modeling framework and maximum-likelihood estimator

In Section 2.1, we describe a data generation process associated with the perturbation model in Fig 1. In Section 2.2, we propose *DirectLikelihood*, a maximum-likelihood estimator with respect to the marginal distribution of the observed variables. *DirectLikelihood* identifies estimates of the unknown perturbation effects, the hidden effects, and the causal relation among the observed variables.

2.1 Modeling framework

We consider a directed acyclic graph \mathcal{D}^* whose $p + h$ nodes correspond to jointly Gaussian and centered¹ random variables $(X, H) \subseteq \mathbb{R}^p \times \mathbb{R}^h$, where X are observable and H are hidden variables. As described in Section 1.1, our methodology is also applicable in the setting where one may be primarily interested in the causal effects of a target variable. As such, we distinguish X_p as the target or response variable. Owing to the joint Gaussianity of (X, H) , the random pair (X, H) satisfies the following (compactified) SCM:

$$X = B^*X + \Gamma^*H + \epsilon. \quad (1)$$

Here, $\epsilon = (\epsilon_1, \epsilon_2, \dots, \epsilon_p)$ are independent Gaussian random variables independent of H where $\epsilon \sim \mathcal{N}(0, \text{diag}(w^{1,*}))$ for some $w^{1,*} \in \mathbb{R}_{++}^p$. The connectivity matrix $B^* \in \mathbb{R}^{p \times p}$ contains zeros on the diagonal and encodes the causal relationship among the observables X , i.e. $B_{k,j}^* \neq 0$ if and only if $j \in \text{PA}_{\mathcal{D}_X^*}(k)$. The p -th row vector $B_{p,\cdot}^*$ encodes the causal parents of the target variable and the magnitude of their effects. The matrix Γ^* in (1) encodes the effects of the hidden variables on the observed variables where $\Gamma_{k,j}^* \neq 0$ if and only if $j \in \text{PA}_{\mathcal{D}_H^*}(k)$. For the sake of generality, we do not immediately put any assumption on the number of hidden variables h or the denseness of their effects.

The compact SCM (1) describes the generating process of X in the observational setting where there are no external perturbations on the system. We next describe how the data generation process alters due to some type of perturbations to the variables (X, H) . We consider perturbations that directly shift the distributions of the random variables by some noise, either acting additively to the system or being a do-intervention eliminating the connections between the perturbed variable and the corresponding parents.

We consider perturbations \mathcal{A} that act either additively to the system or are do-interventions that yield the random pair (X^e, H^e) for each $e \in \mathcal{E}$ satisfying the following SCM:

$$\begin{aligned} X^e &= \mathcal{F}_{\text{do}(e)^c} (B^*X^e + \Gamma^*H^e + \epsilon^e + \delta^e) + \mathcal{F}_{\text{do}(e)} (\delta^e) \\ H^e &\sim \mathcal{N}(0, \Psi^{*,e}), \end{aligned} \quad (2)$$

where for every $e \in \mathcal{E}$, $\epsilon^e \stackrel{\text{dist}}{=} \epsilon$, $(H^e, \delta^e, \epsilon^e)$ are jointly independent, and that the collection $(X^e, H^e, \delta^e, \epsilon^e)$ is independent across e . Further, $\delta^e \in \mathbb{R}^p$ is a Gaussian random vector (independent across the coordinates) that represents the additive perturbations, $H^e \in \mathbb{R}^h$ is a Gaussian random vector that represents the perturbed hidden variables with covariance $\Psi^e \in \mathbb{S}_{++}^h$, and $\text{do}(e) \subseteq \{1, \dots, p\}$ denotes do-locations in the sub-graph of \mathcal{D}_X^* . Finally, $\mathcal{F}_S \in \mathbb{R}^{p \times p}$ is a diagonal matrix with ones corresponding to coordinates inside $S \subseteq \{1, \dots, p\}$ and zeros elsewhere. Notice that ϵ^e, δ^e are in general not identifiable from the sum $\epsilon^e + \delta^e$ in (2); we specify below in Section 2.1.1 an identifiable parametrization for the terms $\epsilon^e + \delta^e$.

The compactified SCM (2) characterizes the distribution among all of the observed variables and encodes system-wide invariances. Specifically, (2) insists that for every $k = 1, 2, \dots, p$, the regression coefficients when regressing X_k^e on the parent sets $\{X_j^e : j \in \text{PA}_{\mathcal{D}_X^*}(k)\}$ and $\{H_l^e : l \in \text{PA}_{\mathcal{D}_H^*}(k)\}$ remain invariant for all environments $e \in \mathcal{E}$. This is a point of departure from instrumental variable techniques or invariant causal prediction in two significant

¹Without loss of generality, we assume that the observed variables are centered.

ways: 1) such methods do not allow for the perturbations on the hidden variables or the target variable X_p (i.e. they assume $H^e \stackrel{\text{dist}}{=} H$ and $\delta_p^e \equiv 0$ for all $e \in \mathcal{E}$) and 2) they only consider “local” invariances arising from the distribution $X_p^e \mid \{(X_j^e, H_l^e) : j \in \text{PA}_{\mathcal{D}_X^*}(k), h \in \text{PA}_{\mathcal{D}_H^*}(k)\}$. The virtue of considering a joint model over all of the variables and exploiting system-wide invariances is that we can propose a maximum-likelihood estimator *DirectLikelihood* which identifies the population DAG structure even with perturbations on the target variable and the hidden variables.

The SCM (2) is similar in spirit to previous modeling frameworks in the literature. The authors [14] consider jointly observational and interventional Gaussian data where the interventions are limited to do-interventions and there are no hidden variables. In the context of (2), this means that $\delta^e \equiv 0$ and $\Gamma^* \equiv 0$. As such, the framework considered in this paper is a substantial generalization of [14]. Further, the backShift [27] procedure considers the linear SCM (2) with the some modifications: i) there are no do-interventions, e.g. $\text{do}(e) = \emptyset$ for all $e \in \mathcal{E}$, ii) there are no perturbations to the hidden variables, i.e. $H^e \stackrel{\text{dist}}{=} H$ for all $e \in \mathcal{E}$, and iii) B^* may be a cyclic directed graph. In addition, the backShift algorithm relies on exploiting invariances of differences of estimated covariance matrices across environments. Our *DirectLikelihood* is more in the “culture of likelihood modeling and inference” and has the advantage that it can cope well with having only a few observations per group or environment. This likelihood perspective also fits much more into the context of inference for mixed models as briefly discussed next.

2.1.1 Model specialization

Clearly, one cannot distinguish the parameters for ϵ^e and δ^e . We thus write, for all $e \in \mathcal{E}$:

$$\epsilon^e + \delta^e \sim \mathcal{N}(0, \text{diag}(w^{e,*})), \quad w^{*,e} \in \mathbb{R}_+^p.$$

Since we are mainly interested in the connectivity matrix B^* , the parameters Γ^* , $w^{e,*}$, $\Psi^{e,*}$ are nuisance parameters and we may simplify the modeling framework by restricting the parameter space for the covariances $\Psi^{e,*}$. Our default proposal is to model the hidden variables as independent and identically distributed across the environments. Specifically, we let $\Psi^{e,*} = \Psi^* + \psi^{e,*}\mathcal{I}$ where $\psi^{e,*} \in \mathbb{R}_+$. Further, without loss of generality, Ψ^* can be taken to be the identity matrix by absorbing its effect on Γ^* via the transformation $\Gamma^* \rightarrow \Gamma^*\Psi^{*1/2}$ so that:

$$\Psi^{e,*} = (1 + \psi^{e,*})\mathcal{I}, \quad \psi^{e,*} \in \mathbb{R}_+.$$

Further, as an additional default setting, we assume that we have access to an observational environment ($e = 1$ without loss of generality) so that:

$$w^{e,*} \succeq w^{1,*}, \quad \psi^{1,*} = 0.$$

Here, the inequality $w^{e,*} \succeq w^{1,*}$ is element-wise.

In the setting where the hidden variables are unperturbed across the environments, one can take $\Psi^{e,*} \equiv \mathcal{I}$ after the transformation $\Gamma(\Psi^{e,*})^{1/2} \rightarrow \Gamma^*$. Fitting to a model with equally distributed perturbations across the coordinates may be attained by the reparametrization $w^{e,*} = w^{1,*} + \zeta^{e,*}\mathbf{1}$ for $\zeta^{e,*} \in \mathbb{R}_+$. In general, other models for the random terms $\epsilon^e + \delta^e$ and H^e are possible. A connection to random effects modeling is discussed next.

2.1.2 Interpretation as mixed-effects linear structural causal model

The framework in (2) bears some similarities to standard random effects mixed models [16]. In particular, random effects mixed models are widely employed to model grouped data across multiple environments, where some parameter components remain fixed and others are random. In the context of our problem, the fixed parameters are the matrices B^*, Γ^* and the random parameters are the shift perturbations δ^e .

For example, we can write for the target variable $Y = X_p$ and for simplicity in the absence of hidden variables: for each environment or group e ,

$$Y^e = X^e\beta + Z^eb^e + \epsilon^e, \quad e = 1, \dots, m, \quad (3)$$

where Y^e, ϵ^e are $n^e \times 1$ vectors, X^e is an $n^e \times p$ design matrix, here $Z^e = \mathcal{I}_{n^e}$, n^e is the sample size within group or environment e , and the variables across e are independent. The correspondence to (2) is as follows: $\epsilon^e \sim \mathcal{N}(0, w_p^{1,*}\mathcal{I}_{n^e})$, $b^e \sim \mathcal{N}(0, v_p^{e,*}\mathcal{I}_{n^e})$ (where $v_p^{e,*} = w_p^{e,*} - w_p^{1,*}$) and $\beta = B_{p,:}^{*T}$. There are three main differences

to standard mixed models. First, the distribution of $b^e \sim \mathcal{N}(0, v_p^{e,*} I_{n^e})$ changes with e and the shrinkage effect across groups is abandoned. Second, we take a multivariate view point for all the variables X_j^e ($j = 1, \dots, p$) in (2): they are all modelled with random effects and can be individually written as in (3), but we allow for dependence among all the p variables. Finally, a difference between our model in (1) and (2) and the standard mixed models is that the group specific random effects, the random parameters δ^e in (2) or the random parameters vector b^e in (3), act in a *dynamic way* on the system: the effects of δ^e are *propagated* through the structural equations; and in practice, the order of propagation is usually unknown.

Thus, our model in (2) leads to a different way of describing group-specific perturbations, calling also for a different likelihood calculation: in fact, as we show, such dynamic perturbations allow to identify the causal structure. The latter is not possible with standard mixed models but due to the connection pointed out above, we refer to our formalization in (2) as "mixed-effects linear structural causal modeling". We believe that the causal inference literature has not much exploited this connection. We argue here that our random effects approach is very useful and practical for modeling perturbation data where the perturbations are believed to propagate further on other variables in the system.

2.2 Scoring DAGs via *DirectLikelihood*

Let \mathcal{D} be a given DAG structure among the observed variables (which we can think of as the restriction \mathcal{D}_X of a DAG among observed and hidden variables). In this section, we score this DAG via the maximum likelihood procedure *DirectLikelihood*. We suppose that there are m environments $|\mathcal{E}| = m$, and for every environment $e = 1, 2, \dots, m$, we have samples of random pairs (X^e, H^e) : $\{X_{(i)}^e\}_{i=1}^{n^e}$ for some positive integer n^e which are IID for each e and independent across e . Thus, since the X^e 's are independent for $e = 1, 2, \dots, m$ and the samples for each environment e are IID, the maximum-likelihood estimator for the DAG structure \mathcal{D} is given by:

$$\begin{aligned} \arg \min_{\substack{B \in \mathbb{R}^{p \times p}, \Gamma \in \mathbb{R}^{p \times \bar{h}} \\ \{\Psi^e\}_{e=1}^m \subseteq \mathbb{S}_{++}^{\bar{h}}, \{w^e\}_{e=1}^m \subseteq \mathbb{R}_{++}^p}} \sum_{e=1}^m \hat{\pi}^e \sum_{i=1}^{n^e} -\log \text{prob} \left(X_{(i)}^e | B, \Gamma, \Psi^e, w^e \right) \\ \text{subject-to } B \text{ compatible with } \mathcal{D}. \end{aligned} \quad (4)$$

Here, $\text{prob} \left(X_{(i)}^e | B, \Gamma, \Psi^e, w^e \right)$ represents the Gaussian likelihood of $X_{(i)}^e$ given parameters B, Γ, Ψ^e, w^e ; $\bar{h} \leq p$; the constraint B compatible with \mathcal{D} ensures that the estimated B has its support restricted to the structure of \mathcal{D} , i.e. $B_{i,j} \neq 0$ if and only if $j \rightarrow i$ in \mathcal{D} ; $\hat{\pi}^e = \frac{n^e}{\sum_{e=1}^m n^e}$; and w^e is a surrogate for the variances of the sum $\delta^e + \epsilon$. It is straightforward to see that the negative log-likelihood $\log \text{prob}(\cdot)$ decouples across the parameters $(B, \Gamma, \{\Psi^e\}_{e=1}^m, \{w_{\text{do}(e)^c}^e\}_{e=1}^m)$ and $\{w_{\text{do}(e)}^e\}_{e=1}^m$. In other words, the structure of the DAG \mathcal{D} only plays a role in the term involving the parameters $(B, \Gamma, \{\Psi^e\}_{e=1}^m, \{w_{\text{do}(e)^c}^e\}_{e=1}^m)$, and we thus focus on that component of the likelihood:

$$\begin{aligned} (\hat{B}, \hat{\Gamma}, \{(\hat{\Psi}^e, \hat{w}^e)\}_{e=1}^m) = \arg \min_{\substack{B \in \mathbb{R}^{p \times p}, \Gamma \in \mathbb{R}^{p \times \bar{h}} \\ \{\Psi^e\}_{e=1}^m \subseteq \mathbb{S}_{++}^{\bar{h}}, \{w^e\}_{e=1}^m \subseteq \mathbb{R}_{++}^p}} \sum_{e=1}^m \hat{\pi}^e \ell(B, \Gamma, \Psi^e, w^e; \text{do}(e), \hat{\Sigma}^e), \\ \text{subject-to } B \text{ compatible with } \mathcal{D} \end{aligned} \quad (5)$$

where

$$\begin{aligned} \ell(\cdot) = \log \det \left(\left[\text{diag}(w^e) + \Gamma \Psi^e \Gamma^T \right]_{\text{do}(e)^c} \right) \\ + \text{trace} \left(\left[\text{diag}(w^e) + \Gamma \Psi^e \Gamma^T \right]_{\text{do}(e)^c}^{-1} \left[(\mathcal{I} - \mathcal{F}_{\text{do}(e)^c} B) \hat{\Sigma}^e (\mathcal{I} - \mathcal{F}_{\text{do}(e)^c} B)^T \right]_{\text{do}(e)^c} \right), \end{aligned}$$

and $\hat{\Sigma}^e$ is the sample covariance matrix of the data $\{X_{(i)}^e\}_{i=1}^{n^e}$. We assume that the location of the do-interventions are known so that the input to the program (5) are the sample covariance matrices $\hat{\Sigma}^e$, the do-intervention locations $\text{do}(e)$, and the estimate \bar{h} for the number of hidden variables. We note that the *DirectLikelihood* estimator can be specialized to different modeling options based on appropriate reparametrization of the nuisance parameters Ψ^e, w^e in (5). For example, in our default setting of IID hidden variables with the environment $e = 1$ being observational

(see Section 2.1.1), we add the following constraints to (5):

$$\begin{aligned}\Psi^e &= (1 + \psi^e)\mathcal{I} \text{ with } \psi^e \in \mathbb{R}_+ \text{ for } e = 1, \dots, m \\ w^e &\succeq w^1 \text{ for } e = 2, \dots, m; \psi^1 = 0.\end{aligned}$$

Given estimates $(\hat{B}, \hat{\Gamma}, \{\hat{\Psi}^e\}_{e=1}^m, \{\hat{w}^e\}_{e=1}^m)$, our score for the DAG \mathcal{D} is:

$$\text{score}_\lambda(\mathcal{D}) = \sum_{e=1}^m \hat{\pi}^e \ell(\hat{B}, \hat{\Gamma}, \hat{\Psi}^e, \hat{w}^e; \text{do}(e), \hat{\Sigma}^e) + \lambda \|\text{moral}(\mathcal{D})\|_{\ell_0}. \quad (6)$$

Here, $\text{moral}(\mathcal{D})$ denotes the moralization of \mathcal{D} which forms an undirected graph of \mathcal{D} by adding edges between nodes that have common children, $\lambda > 0$ is a regularization parameter, and $\lambda \|\text{moral}(\mathcal{D})\|_{\ell_0}$ is akin to the Bayesian Information Criterion (BIC) score that prevents overfitting by incorporating the denseness of the moral graph of \mathcal{D} in the likelihood score. In principle, a collection of DAGs can each be individually scored via (6) to find the best fit to the data. We remark that regularization terms controlling for complexity of estimated DAGs are commonly employed in structural causal learning (see [9] and the references therein). A classically known fact is that in a single environment setting, the moral graph of the DAGs in the Markov equivalence class have the same cardinality [32]. In the context of this paper with perturbations, incorporating the sparsity of the moral graph plays a central role in our theoretical analysis for proving identifiability; see Section 3.1 for more discussion.

In comparison to the *DirectLikelihood* procedure, `backShift` [27] fits the SCM (2) (with some restrictions outlined in Section 2.1) by performing joint diagonalization to the difference of sample covariance matrices. *DirectLikelihood* allows for much more modeling flexibility. First, in contrast to `backShift` where the hidden effects are subtracted by computing the difference of covariances, *DirectLikelihood* explicitly models these effects. This feature of *DirectLikelihood* enables the possibility of perturbations to the hidden variables and a manner to control the number of estimated hidden variables (as opposed to arbitrary number of hidden variables with `backShift`). We discuss in Section 3 that controlling the number of hidden variables may lead to identifiability using *DirectLikelihood* with a single interventional environment, whereas `backShift` is guaranteed to fail. Second, *DirectLikelihood* also models the perturbation magnitudes in each environment, allowing for the flexibility of constraining the perturbation magnitudes to improve estimation accuracy. Finally, *DirectLikelihood* allows to pool information over different environments e for the parameter B of interest: this enable *DirectLikelihood* to be used with only a few sample points per environment.

2.3 Beyond Gaussianity

The *DirectLikelihood* estimator (5) fits a Gaussian perturbation model (2) to the data. However, the perturbation data of the observed variables may be non-Gaussian but satisfy the linear SCM (2). In particular, the random variables H^e, δ^e may be non-Gaussian while still inducing a linear relationship with the observed variables X^e . Nonetheless, since the *DirectLikelihood* estimator only operates on second moments, one may still use the *DirectLikelihood* procedure to find the best scoring DAGs and the associated connectivity matrices without compromising identifiability guarantees as shown in Section 3, still implying corresponding estimation consistency. Further, we empirically explore the robustness of the *DirectLikelihood* procedure to non-Gaussianity as well as other model misspecifications via numerical experiments in Section 6.

3 Theoretical properties: identifiability via *DirectLikelihood*

We next investigate the theoretical properties of the *DirectLikelihood* procedure. The main theorem in this section (Theorem 1) considers the general setting with perturbed latent variables and establishes identifiability properties under some population assumptions. Subsequently, Theorem 2 and Theorem 3 in Section 3.2 analyze *DirectLikelihood* under specializations of the modeling framework, namely unperturbed hidden variables and no hidden variables, respectively. Throughout, the notation with $*$ indicates the true underlying population objects which we aim to estimate from data.

Setup: We consider the perturbation model in (2) with a population connectivity matrix $B^* \in \mathbb{R}^{p \times p}$, hidden effects coefficient matrix $\Gamma^* \in \mathbb{R}^{p \times h}$. For every environment e , the random vector H^e has a covariance matrix $\Psi^{e,*} \in \mathbb{S}_{++}^h$ and the random vector $\epsilon^e + \delta^e$ has a diagonal covariance matrix $\text{diag}(w^{e,*})$ for $w^{e,*} \in \mathbb{R}_+^p$. In the subsequent discussion, we allow for H^e, δ^e , and ϵ to be non-Gaussian random vectors. As prescribed in Section 2.1.1

but not requiring Gaussianity, we assume that the hidden variables are independent and identically distributed (our theoretical results can be extended to the setting with non-IID latent variables), i.e. $\Psi^{e,*} = (1 + \psi^{e,*})\mathcal{I}$ with $\psi^{e,*} \in \mathbb{R}_+$. We assume that for every environment $e = 1, 2, \dots, m$, we have IID data $\{X_{(i)}^e\}_{i=1}^{n_e} \subseteq \mathbb{R}^p$ where $e = 1$ is an observational environment with no perturbations (although the results can be readily extended when there are perturbations in all environments). To score a given DAG \mathcal{D} , we consider the modified *DirectLikelihood* estimator (5) in population:

$$\begin{aligned} & \min_{\substack{B \in \mathbb{R}^{p \times p}, \Gamma \in \mathbb{R}^{p \times h} \\ \{(\psi^e, w^e)\}_{e=1}^m \subseteq \mathbb{R}_+ \times \mathbb{R}_+^p}} \sum_{e=1}^m \pi^{e,*} \ell(B, \Gamma, (1 + \psi^e)\mathcal{I}, w^e; \text{do}(e), \Sigma^{e,*}). \\ & \text{subject-to} \quad B \text{ compatible with } \mathcal{D} \ ; \ \psi^e \leq C_\psi \text{ for } e = 1, \dots, m \\ & \quad \quad \quad \psi^1 = 0 \ ; \ w^e \succeq w^1 \text{ for } e = 2, \dots, m. \end{aligned} \tag{7}$$

Comparing (7) to the *DirectLikelihood* estimator (5), the reparametrization $\Psi^e \rightarrow (1 + \psi^e)\mathcal{I}$ is to account for the hidden variables being IID and the constraints $\psi_1 = 0$ and $w^e \succeq w^1$ for $e = 2, \dots, m$ account for $e = 1$ being an observational environment. Further, the constraint $\|\psi\|_\infty \leq C_\psi$ bounds the strength of the hidden perturbations for some user-specified parameters $C_\psi \geq 0$.

We consider optimally scoring DAG(s) with their associated connectivity matrices:

$$\mathcal{D}_{\text{opt}} = \arg \min_{\text{DAG } \mathcal{D}} \text{score}_{\lambda=0}(\mathcal{D}) \ ; \ B_{\text{opt}} : \text{ associated connectivity matrix(ces)}. \tag{8}$$

Here, $\text{score}_{\lambda=0}(\mathcal{D})$ is the achieved minimum in (7). It is the analogue of (6) but using the population covariance matrix $\Sigma^{e,*}$ and the population optimizers from (7). The sample *DirectLikelihood* procedure replaces $\Sigma^{e,*}$ and $\pi^{e,*}$ in (7) with the population covariance matrix $\hat{\Sigma}^e$ and the mixture coefficients $\hat{\pi}^e$, respectively. Further, in the sample setting, the regularization parameters λ in the score evaluation (6) is set to scale with the BIC score. Using the sample quantities as described above we denote by

$$\hat{\mathcal{D}}_{\text{opt}}, \hat{B}_{\text{opt}} \tag{9}$$

the optimal scoring DAGs and connectivity matrices in the sample version. Our objective is to demonstrate that under some assumptions, $\mathcal{D}_{\text{opt}} = \mathcal{D}_X^*$, $B_{\text{opt}} = B^*$, and in the limit of sample sizes for all environments tending to infinity, $\hat{\mathcal{D}}_{\text{opt}} \rightarrow \mathcal{D}_X^*$ and $\hat{B}_{\text{opt}} \rightarrow B^*$ in probability.

Our consistency results are in the general setting where there are perturbations on the hidden variables require an assumption on the hidden variable effects, dubbed *hidden spuriousness*, that is formalized below:

Definition 1 (*hidden spuriousness* for $e \in \mathcal{E}$). *The random variables (X^e, H^e) satisfy hidden spuriousness if there exists a pair k, l such that:*

$$\rho(X_k^e, X_l^e | X_{\setminus\{k,l\}}^e, H^e) = 0 \ \& \ \rho(X_k^e, X_l^e | X_{\setminus\{k,l\}}^e) \neq 0.$$

In words, (1) states that the hidden variables induce “some” confounding dependencies among the observed variables in environment $e \in \mathcal{E}$. In comparison, the hidden denseness assumption needed for consistency of the two stage deconfounding procedures [4, 11] require that the hidden variables induce “many” confounding dependencies. As such, *hidden spuriousness* is a strictly (and often substantially) weaker condition than the denseness assumption required for the success of the two stage deconfounding. We investigate whether *DirectLikelihood* is able to identify the population connectivity matrix B^* under this weaker condition, and answer in the affirmative under appropriate conditions on the strength and heterogeneity of the interventions. We provide two sets of assumptions that lead to identifiability. The first set requires two interventional environments that have sufficiently large interventions on the observed variables, and the second set requires two interventional environments with one interventional environment consisting of much stronger interventions on the observed variables than the other interventional environment. The two set of assumptions are described below where the observational environment is denoted by $e = 1$ and the two interventional environments are denoted by $e = 2, 3$:

Assumption 1 – no do interventions: $\text{do}(e) = \emptyset$ for $e = 2, 3$

Assumption 2 – the mixture effects are non-vanishing: $\pi^{e,*} > 0$ for $e = 1, 2, 3$

Assumption 3 – heterogeneity of perturbations for $e = 2, 3$:

$$\frac{w_k^{2,*} - (1 + \psi^{2,*})w_k^{1,*}}{w_l^{2,*} - (1 + \psi^{2,*})w_l^{1,*}} \neq \frac{w_k^{3,*} - (1 + \psi^{3,*})w_k^{1,*}}{w_l^{3,*} - (1 + \psi^{3,*})w_l^{1,*}} \text{ for all } k \neq l \quad (10)$$

Assumption 4 – *hidden spuriousness* in Definition 1 for environments $e = 2, 3$

Assumption 5 – sufficiently large interventions on variables for $e = 2, 3$:

$$\frac{\min_k (w_k^{e,*})^2}{\max_k w_k^{e,*}} > 8\kappa^*(1 + 2C_\psi)^2(1 + \|w^{1,*}\|_\infty)(1 + \|\Gamma^*\|_2^2 + \|\Gamma^*\|_2^4)$$

or

Assumption 6 – no do interventions: $\text{do}(e) = \emptyset$ for $e = 2, 3$

Assumption 7 – the mixture effects are non-vanishing: $\pi^{e,*} > 0$ for $e = 1, 2, 3$

Assumption 8 – heterogeneity of perturbations for $e = 2, 3$:

$$\frac{w_k^{3,*} - (1 + \psi^{3,*})w_k^{1,*}}{w_l^{3,*} - (1 + \psi^{3,*})w_l^{1,*}} \neq \frac{w_k^{3,*} - \frac{1 + \psi^{3,*}}{1 + \psi^{2,*}}w_k^{2,*}}{w_l^{3,*} - \frac{1 + \psi^{3,*}}{1 + \psi^{2,*}}w_l^{2,*}} \text{ for all } k \neq l \quad (11)$$

Assumption 9 – *hidden spuriousness* in Definition 1 for environments $e = 3$

Assumption 10 – sufficiently large interventions on variables in S for $e = 3$:

$$\frac{\min_k (w_k^{e,*})^2}{\max_k w_k^{e,*}} > 8\kappa^*(1 + 2C_\psi)^2(1 + \|w^{2,*}\|_\infty)(1 + \|\Gamma^*\|_2^2 + \|\Gamma^*\|_2^4)$$

where the quantity $\kappa^* \equiv \frac{1 + \max_i \|B_{:,i}^*\|_2^2}{1 + \min_i \|B_{:,i}^*\|_2^2}$ in Assumption 5 of (10) and Assumption 10 of (11). Assumptions 1-5 in (10) and 6-10 in (11) impose conditions on the population quantities associated with the environments $e = 1, 2, 3$. In particular, Assumption 1 in (10) and Assumption 6 in (11) require that there are at least two environments with shift interventions, but additional do-interventions would be allowed (treating them as additional environments); Assumption 2 in (10) and Assumption 7 in (11) require that the contribution for each environment does not vanish in the large data limit; Assumption 3 in (10) and Assumption 8 in (11) ensure that the perturbations are heterogeneous. In principle, the interventions on the observed variables in the environments $e = 2, 3$ may come from identical distributions (i.e. $w^{2,*} = w^{3,*}$) or one of them being even zero (i.e. $w^{2,*} = w^{1,*}$) with different hidden variable perturbations (i.e. $\psi^{2,*} \neq \psi^{3,*}$) without compromising Assumption 3 in (10) or Assumption 8 in (11). Additionally, one can show that if the parameters $w^{3,*}, w^{2,*}, w^{1,*}$ and $\psi^{2,*}, \psi^{3,*}$ are drawn from continuous distributions, Assumption 3 in both (10) and (11) are satisfied almost surely. Assumption 4 in (10) and (11) insists that the *hidden spuriousness* in (1) is satisfied so that the hidden variables induce at least a single spurious dependency among the observed variables. Finally, Assumption 5 in (10) and Assumption 10 in (11) requires that the perturbations on the observed variables are sufficiently large. This is akin to strong instruments assumption in the instrumental variables literature [1].

Given Assumptions 1-5 in (10) or Assumptions 6-10 in (11), we first analyze the theoretical properties of the population *DirectLikelihood* procedure.

Theorem 1 (Identifiability in population: perturbed hidden variables). *Suppose that the user-specified parameters \bar{h} and C_ψ in (7) are chosen conservatively so that $\bar{h} \geq \dim(H)$ and $C_\psi \geq \psi^{e,*}$ for all $e = 1, 2, \dots, m$. Under Assumptions 1-5 in (10) or Assumptions 6-10 in (11), the following are satisfied for \mathcal{D}_{opt} in (8):*

1. $\mathcal{D}_X^* \in \mathcal{D}_{\text{opt}}$ and any other optimum $\mathcal{D} \in \mathcal{D}_{\text{opt}}$ satisfies: $\text{moral}(\mathcal{D}_X^*) \subseteq \text{moral}(\mathcal{D})$.
2. The optimum of $\arg \min_{D \in \mathcal{D}_{\text{opt}}} \|\text{moral}(D)\|_{\ell_0}$ is unique and equal to \mathcal{D}_X^* . Further, the associated connectivity matrix is equal to B^* .

The proof sketch of Theorem 1 is provided in Section 3.1 and the full proof is presented in the supplementary material Section A.1. The first assertion in Theorem 1 states that the moral graph of any optimum $\mathcal{D} \in \mathcal{D}_{\text{opt}}$ of the *DirectLikelihood* procedure is a superset of the moral graph of \mathcal{D}^* , and the second assertion states that the connectivity matrices yielding the sparsest moral graphs among the optima are unique and equal to B^* . These

statements do not guarantee recovering the other model parameters, viewed here as nuisance part, including Γ^* , and $\{(\psi^{e,*}, w^{e,*})\}_{e=1}^m$. However, under additional assumptions namely: $\bar{h} = \dim(H)$ and the incoherence of the subspace $\text{col-space}(\Gamma^*)$, recovery of $\Gamma^*\Gamma^{*T}$ and $\{(\psi^{e,*}, w^{e,*})\}_{e=1}^m$ can be shown.

We note that Assumptions 1-5 in (10) or Assumptions 6-10 in (11) are sufficient conditions for identifiability and are generally not necessary. As an example, we show in supplementary material Section A.2 that identifiability cannot be achieved with only a single interventional environment if $\bar{h} = p$ (e.g. most conservative choice for the number of latent variables). However, we also demonstrate that if $\bar{h} < p$, *DirectLikelihood* will attain identifiability under certain configurations of model parameters (i.e dense hidden effects with sparse population DAG \mathcal{D}_X^*). Thus, Assumptions 1-5 in (10) or 6-10 in (11) serve as protection for arbitrary population DAG structure and a class of model parameters. We believe that relaxing these assumptions while retaining identifiability guarantees is an interesting direction for future research.

The virtue of incorporating the regularization term $\lambda\|\mathcal{D}\|_{\ell_0}$ in (6) is that in the large data limit, this penalty term encourages sparser moral graphs. Thus, in conjunction with the results of Theorem 1, we demonstrate that in the large data limit, the set $\hat{\mathcal{D}}_{\text{opt}}$ and \hat{B}_{opt} asymptotically converge to \mathcal{D}_X^* and B^* , respectively. To appeal to standard empirical process theory results, we constrain the parameter space to be compact as described in the corollary below:

Corollary 1 (Asymptotic consistency for perturbed hidden variables). *Consider the sample version of the DirectLikelihood procedure in (7) with the compactness constraints $\max\{1/\min_k w_k^e, \|B\|_2\} \leq C_{\text{comp}}$ for every every $e = 1, 2, \dots, m$ where $C_{\text{comp}} > \max\{1/\min_k w_k^{e,*}, \|B^*\|_2\}$ so that the true parameters are in the feasible region. Further, let $\lambda \sim \mathcal{O}(\log(\sum_{e=1}^m n^e)/\sum_{e=1}^m n^e)$ in (6). Under the conditions in Theorem 1, the following are satisfied for $\hat{\mathcal{D}}_{\text{opt}}$ and \hat{B}_{opt} in (9): $\hat{\mathcal{D}}_{\text{opt}} \rightarrow \mathcal{D}_X^*$ and $B_{\text{opt}} \rightarrow B^*$, in probability, as $n^e \rightarrow \infty$ for $e = 1, 2, 3$.*

The proof of Corollary 1 is a straightforward consequence of Theorem 1 and left out for brevity. The combined results of Theorem 1 and Corollary 1 state that under perturbations that are sufficiently different across environments and the *hidden spuriousness* condition, two interventional environments suffice for consistent estimation.

Remark 1: Assumptions 1-5 in (10) and (11) needed for identifiability suggest that perturbations on the hidden variables can improve identifiability. Specifically, the perturbations on the observed variables in one interventional environment may be statistically identical to another environment or even be completely equal to zero and still preserve identifiability as long as the hidden variables have been perturbed.

Remark 2: As described in Section 2.1, the perturbation model (2) offers flexibility with respect to many components of the model such as the structure of the perturbations on the observed or hidden variables. In particular, one may fit to data the perturbation model (2) where the perturbation magnitudes are equal in magnitude across the coordinates, e.g. $\text{diag}(w^{e,*}) \propto \mathcal{I}$. We demonstrate in the supplementary material Section A.3 that *DirectLikelihood*, under Assumptions similar to (10) or (11), provides consistent estimators in this setting. Thus, in principle one may have only two additional perturbation parameters per environment: a scalar for the hidden variables and a scalar for the observed variables. As a point of contrast, in the setting where the perturbations among the observed variables may vary, there are $p + 1$ new variables for each environment. The substantial reduction in the number of parameters can lead to better statistical properties in practice.

3.1 Proof sketch of Theorem 1

We sketch the main proof idea of Theorem 1 with Assumptions 1-5 in (10). The proof strategy with Assumptions 6-10 in (11) is similar. It is straightforward to see that any optimal connectivity matrix $B \in B_{\text{opt}}$ of the population *DirectLikelihood* procedure satisfies the following condition for some $\{(\psi^e, w^e)\}_{e=1}^m \subset \mathbb{R}_+ \times \mathbb{R}_{++}^p$, $\Gamma \in \mathbb{R}^{p \times \bar{h}}$ with $\psi^e \leq C_\psi$ for all $e = 1, 2, \dots, m$:

$$\begin{aligned} \Sigma^{e,*} &= (\mathcal{I} - \mathcal{F}_{\text{do}(e)^c} B)^{-1} (\text{diag}(w^e) + [(1 + \psi^e)\Gamma\Gamma^T]_{\text{do}(e)^c}) (\mathcal{I} - \mathcal{F}_{\text{do}(e)^c} B)^{-T} \\ &\text{for all } e = 1, 2, \dots, m \text{ where } \pi^{e,*} > 0. \end{aligned} \quad (12)$$

In addition to the population parameters $(B^*, \Gamma^*, \{(\psi^{e,*}, w^{e,*})\}_{e=1}^m)$, suppose there is another collection of optimal parameters $(\tilde{B}, \tilde{\Gamma}, \{(\psi^e, \tilde{w}^e)\}_{e=1}^m)$ satisfying (12). Focusing on the environments $e = 1, 2, 3$, Assumptions 5 implies that the matrix $\Sigma^{e,*} - (1 + \tilde{\psi}^e)\Sigma^{1,*}$ is invertible for $e = 2, 3$, where the inverse can be expressed as:

$$(\Sigma^{e,*} - (1 + \tilde{\psi}^e)\Sigma^{1,*})^{-1} = (\mathcal{I} - B^*)^T (D^e - L^e) (\mathcal{I} - B^*) = (\mathcal{I} - \tilde{B})^T \tilde{D}^e (\mathcal{I} - \tilde{B}).$$

Here, $\tilde{D}^e = \text{diag}(\tilde{w}^e - \tilde{w}^1(1 + \tilde{\psi}^e))$. Moreover, under Assumptions 3 and 5, $D^e, \tilde{w}^e \in \mathbb{S}^p$ are invertible diagonal matrices with $\frac{D_{k,k}^2}{D_{l,l}^2} \neq \frac{D_{k,k}^3}{D_{l,l}^3}$ for all $k \neq l$. Further, $L^e \in \mathbb{S}^p$ is identically zero if $\psi^{e,*} = \tilde{\psi}^e$, and a rank- h matrix otherwise. The nonzero entries of $(\mathcal{I} - B^*)^T D^e (\mathcal{I} - B^*)$ and $(\mathcal{I} - \tilde{B})^T \tilde{D}^e (\mathcal{I} - \tilde{B})$ encode the moral graph associated with B^* and \tilde{B} , respectively. By Assumption 5, the magnitude of any nonzero entry of the matrix $(\mathcal{I} - B^*)^T D^e (\mathcal{I} - B^*)$ is greater than the maximal nonzero entry of $(\mathcal{I} - B^*)^T L^e (\mathcal{I} - B^*)$. This proves the first component of Theorem 1.

We next sketch the proof of the second component. If $L^e \neq 0$, by Assumption 4, there exists a pair of indices (k, l) such that: $[(\mathcal{I} - B^*)^T L^e (\mathcal{I} - B^*)]_{k,l} \neq 0$ and $[(\mathcal{I} - B^*)^T D^e (\mathcal{I} - B^*)]_{k,l} = 0$. This would imply that $\text{moral}(B^*) \subset \text{moral}(\tilde{B})$. Since we are interested in connectivity matrices that yield the sparsest moral graph, we conclude that $L^e = 0$. We now have established that \tilde{B} yields the same moral graph as B^* and satisfies for $e = 2, 3$:

$$(\mathcal{I} - B^*)^T D^e (\mathcal{I} - B^*) = (\mathcal{I} - \tilde{B})^T \tilde{D}^e (\mathcal{I} - \tilde{B}).$$

Since D^2, D^3 are non-singular matrices with the property that $\frac{D_{k,k}^2}{D_{l,l}^2} \neq \frac{D_{k,k}^3}{D_{l,l}^3}$ for all $k \neq l$, one can then show via algebraic manipulations that $\tilde{B} = B^*$.

3.2 Specializations: unperturbed hidden variables and no hidden confounding

We first analyze the identifiability guarantees of the *DirectLikelihood* procedure when the hidden variables remain unperturbed across the environments, i.e. the perturbation \mathcal{A} does not point to H in Fig 1. Specifically, we consider the setup described in the beginning of Section 3 with the modification that $\psi^{e,*} = 0$. Thus, we also modify the *DirectLikelihood* estimator (7) by setting $\psi \equiv 0$. We further consider an arbitrary hidden effects matrix Γ^* , where the two-stage deconfounding procedure will not perform well, since hidden denseness may not be satisfied. We demonstrate on the other hand, that the under sufficient interventions, the connectivity matrix that attains the optimum score via *DirectLikelihood* in population is unique and equal to B^* .

Theorem 2 (Identifiability in population: unperturbed hidden variables). *Let $\bar{h} \geq h$ in the DirectLikelihood estimator (7). Letting $S \subseteq \{1, 2, \dots, p\}$ encode the location of perturbations, suppose that Assumption 3 in (10) is modified to $\frac{w_k^{2,*} - w_k^{1,*}}{w_l^{2,*} - w_l^{1,*}} \neq \frac{w_k^{3,*} - w_k^{1,*}}{w_l^{3,*} - w_l^{1,*}}$ for all $k, l \in S, k \neq l$ and Assumption 5 in (10) is modified to $w_k^{e,*} > w_k^{1,*}$ for $e = 2, 3$ and all $k \in S$. Then, under Assumptions 1,2 in (10) and modified Assumptions 3 and 5, we have for \mathcal{D}_{opt} and B_{opt} as in (8):*

- (a) $\mathcal{D}_{opt} = \mathcal{D}_X^*$ and $B_{opt} = B^*$ if $S = \{1, \dots, p\}$.
- (b) Any optimum $B \in B_{opt}$ satisfies $B_{p,:} = B_{p,:}^*$ for the sets $\text{ANC}(p) \subseteq S$ or $\text{DES}(p) \cup p \subseteq S$.
- (c) $\bar{B} = \arg \min_{B \in B_{opt}} \|B\|_{\ell_0}$ satisfies $\bar{B}_{p,:} = B_{p,:}^*$ if $\text{PA}(p) \cup p \subseteq S$ and additionally \mathcal{D}_X^* is faithful to the distribution of $X|H$.

The proof of Theorem 2 is similar in nature to that of Theorem 1 and can be found in the supplementary material Section A.4. Further, analogous to Corollary 1, one can readily show the large limit convergence of the population *DirectLikelihood* to the sample *DirectLikelihood*, although we omit this for brevity.

Remark 2: The conditions needed for identifiability of the unperturbed hidden variable setting (Theorem 2) differ from the perturbed setting (Theorem 1) in multiple ways. First, there are no conditions on the strength of perturbations on the observed variables. Further, the hidden coefficient matrix Γ^* may be arbitrary without needing conditions like *hidden spuriousness*. Finally, the setting with unperturbed latent variables requires two interventional environments where all observed variables are perturbed, whereas the setting with perturbed hidden variables only requires a single environment with perturbations on all the observed variables and another environment where the hidden variables are perturbed.

Remark 3: Theorem 2(a) is similar in nature to the backShift procedure [27]. Nonetheless, *DirectLikelihood* provides additional flexibility such as controlling the number of latent variables, incorporating do-interventions, and structure in the strength of shift interventions that lead to more desirable statistical properties. As an example, a necessary condition for identifiability using the backShift procedure is that there are at least two interventional environments. We demonstrate in supplementary material Section A.2 that this is also a necessary condition with

DirectLikelihood if $\bar{h} = p$. However, under $\bar{h} < p$, *DirectLikelihood* may attain identifiability with only a single interventional environment. As another example, a single interventional environment consisting of the same magnitude perturbation across the coordinates is sufficient for consistency (see Section A.4 of the supplementary material for the theoretical statement).

We next focus on the setting where there is no hidden confounding, i.e. H does not point to the covariates X in Fig 1. We consider the setup described in the beginning of Section 3 with the modification $\Gamma^* \equiv 0$. Thus, we also modify the *DirectLikelihood* estimator (7) by setting $\Gamma \equiv 0$. Below, we provide identifiability guarantees for the *DirectLikelihood* scoring procedure:

Theorem 3 (Identifiability in population: no hidden variables). *Suppose that Assumption 1 and 2 in (10) are modified to only be valid for environments $e = 1, 2$. Further, letting $S \subseteq \{1, 2, \dots, p\}$ encode the location of perturbations, Assumption 3 is modified to $\frac{w_k^{2,*}}{w_l^{2,*}} \neq \frac{w_k^{1,*}}{w_l^{1,*}}$ for all $k, l \in S, k \neq l$ and Assumption 5 to $w_k^{2,*} > w_k^{1,*}$ for all $k \in S$. Then, under these modified Assumptions 1, 2, 3, 5, we have for \mathcal{D}_{opt} and B_{opt} as in (8):*

- (a) $\mathcal{D}_{opt} = \mathcal{D}_X^*$ and $B_{opt} = B^*$ if $S = \{1, \dots, p\}$.
- (b) Any optimum $B \in B_{opt}$ satisfies $B_{p,:} = B_{p,:}^*$ if $ANC(p) \subseteq S$ or $DES(p) \cup p \subseteq S$.
- (c) $\bar{B} = \arg \min_{B \in B_{opt}} \|B\|_{\ell_0}$ satisfies $\bar{B}_{p,:} = B_{p,:}^*$ if $PA(p) \cup p \subseteq S$ and additionally \mathcal{D}_X^* is faithful to the distribution of X .

Remark 5: The proof of Theorem 3 is shown in the supplementary material Section A.4. Notice that unlike the settings with hidden confounding (perturbed or unperturbed), one interventional environment suffices for consistent estimation. Furthermore, as in the case of hidden confounding, in principle, the shift interventions may be independent and identically distributed without compromising the identifiability results.

4 Connections to distributional robustness

Recent works have demonstrated an intrinsic connection between distributional robustness and causal inference. Specifically, in the setting where the target variable is not directly perturbed and there is no hidden confounding, the causal parameter $B_{p,:}^*$ linking the covariates $X_{\setminus p}$ to the target variable X_p in the SCM (2) satisfies the following max-risk optimization problem:

$$B_{p,:}^* = \min_{\substack{\beta \in \mathbb{R}^p \\ \beta_p = 0}} \max_{\substack{\mathcal{P}_e \in \mathcal{P} \\ X^e \sim \mathcal{P}_e}} \|X_p^e - X^e \beta\|_2^2, \quad (13)$$

for a certain perturbation distribution class \mathcal{P} consisting of distributions \mathbb{P}_e indexed by environments e [3]. In particular, the causal coefficients $B_{p,:}^*$ are solutions to a robust optimization problem subject to distributional changes to the system which do not act directly on X_p . Given access to exogenous variables or different environments, [26] allow for non-perturbed latent variables and possibly direct action of change on the target of interest, and prove a relation between the causal parameters and a particular robust optimization program.

In this section, we demonstrate that the joint causal parameters B^* are solutions to a certain max-risk problem in the setting where there may be perturbations to all the variables including the hidden variables, further strengthening the connection between causal inference and distributional robustness. We consider the following perturbation distribution class parameterized by the quantities $C_\zeta, C_\psi \geq 0$:

$$\mathcal{P}_{C_\zeta, C_\psi} = \left\{ \text{distribution } \mathcal{P}_e \text{ over random pairs } (X^e, H^e) \text{ satisfying default SCM (2) and} \right. \\ \left. w^{e,*} = w^{1,*} + \zeta^{e,*} \mathbf{1} \text{ with } \zeta^{e,*} \in [0, C_\zeta], \psi^{e,*} \in [0, C_\psi], \text{do}(e) = \{\emptyset\} \right\},$$

where the default SCM is the setting with IID hidden variables, i.e. $\Psi^{e,*} = (1 + \psi^{e,*})\mathcal{I}$. Recall that the sum $\epsilon^e + \delta^e$ in the SCM (2) is distributed as follows: $\epsilon^e + \delta^e \sim \mathcal{N}(0, \text{diag}(w^{e,*}))$. The constraints on $w^{e,*}$ ensure that the perturbations on the observed variables are IID with magnitude less than a pre-specified level C_ζ ; the constraints on ψ_e^* ensure that the perturbations on the hidden variables have magnitude less than a pre-specified level of

C_ψ ; finally the constraint $\text{do}(e) = \{\emptyset\}$ ensures that there are no do-interventions. We note that the distributions inside \mathcal{P} are specified by parameters that are invariant, namely the population connectivity matrix B^* , the hidden effects matrix Γ^* , and noise variable ϵ with variance of its coordinates encoded in $w^{1,*}$. We consider the following worst-case optimization program that identifies parameters B, Γ, v that are robust to perturbations from the class $\mathcal{P}_{C_\zeta, C_\psi}$:

$$(B_{\text{robust}}, \Gamma_{\text{robust}}, w_{\text{robust}}^1) = \arg \min_{\substack{B \text{ is a DAG} \\ \Gamma \in \mathbb{R}^{p \times \bar{h}}, w^1 \in \mathbb{R}_{++}^p}} \max_{\substack{\mathcal{P}_e \in \mathcal{P}_{C_\zeta, C_\psi} \\ (X^e, H^e) \sim \mathcal{P}_e}} \text{KL}(\Sigma^{e,*}, \Sigma_{B, \Gamma, w^1}(\bar{\zeta}^e, \bar{\psi}^e)), \quad (14)$$

where $\Sigma_{B, \Gamma, w^1}(\cdot, \cdot)$ is an estimated covariance model with definition shown below and KL is the Gaussian Kullback-Leibler divergence between the estimated and population covariance models. Here, $\bar{\zeta}^e, \bar{\psi}^e \in \mathbb{R}_+$ are estimates for the nuisance perturbation parameters $\zeta^{e,*}, \psi^{e,*}$ that vary across the perturbation distributions. For a given B, Γ, w^1 , the quantities $(\bar{\zeta}^e, \bar{\psi}^e)$ are obtained by finding the best fit to data: $(\bar{\zeta}^e, \bar{\psi}^e) = \arg \min_{0 \leq \zeta^e \leq C_\zeta, 0 \leq \psi^e \leq C_\psi} \text{KL}(\Sigma^{e,*}, \Sigma_{B, \Gamma, w^1}(\zeta^e, \psi^e))$ where $\Sigma_{B, \Gamma, d}(\zeta^e, \psi^e) = (\mathcal{I} - \mathcal{F}_{\text{do}(e)c} B)^{-1} (\text{diag}(w^1) + \zeta^e \mathcal{I}) + (1 + \psi^e) \Gamma \Gamma^T (\mathcal{I} - \mathcal{F}_{\text{do}(e)c} B)^{-T}$ is the covariance specified by the model parameters.

In comparison to (13), the risk in (14) is measured jointly over the entire collection of observed variables (via the covariance matrix). As observed previously, this system-wide perspective is crucial for allowing perturbations on all of the variables. The following theorem connects the max-risk solutions B_{robust} to the causal parameter B^* .

Theorem 4. *Suppose that the estimated number of latent variables \bar{h} in (14) is chosen conservatively, i.e. $\bar{h} \geq \text{dim}(H)$. Let the maximum perturbation size on the observed variables in the perturbation class satisfy $C_\zeta \geq \kappa^* (1 + 2C_\psi)^2 (1 + \|w^{1,*}\|_\infty) (1 + \|\Gamma^*\|_2^2 + \|\Gamma^*\|_2^4)$ where $\kappa^* \equiv \frac{1 + \max_i \|B_{:,i}^*\|_2}{1 + \min_i \|B_{:,i}^*\|_2}$. Suppose there exists a perturbation distribution $\mathcal{P}_e \in \mathcal{P}_{C_\zeta, C_\psi}$ with parameters $\zeta^{e,*} = C_\zeta, \psi^{e,*} \neq 0$ such that the random pairs (X^e, H^e) drawn from this distribution satisfy the hidden spuriousness assumption in (1). Then:*

1. Any optimal connectivity matrix $B \in B_{\text{robust}}$ satisfies $\text{moral}(B^*) \subseteq \text{moral}(B)$
2. The optimum of $\arg \min_{B \in B_{\text{robust}}} \|\text{moral}(B)\|_{\ell_0}$ is unique and equal to B^* .

Remark 6: The proof of Theorem 4 is presented in the supplementary material Section A.5. This theorem result states that the causal parameter B^* is a solution to a max-risk optimization problem over a certain perturbation class (and produces the sparsest moral graph among the optimum), establishing a fundamental relation between causality and distributional robustness. Further, under similar assumptions as required in Theorem 2 and Theorem 3, analogous connections can be established for the setting with unperturbed and no hidden variables, respectively.

5 Computing the *DirectLikelihood* estimates

Solving the *DirectLikelihood* estimator (5) for a DAG \mathcal{D} is a challenging task, as the problem is non-convex over the decision variables $B, \Gamma, \{\Psi^e\}_{e=1}^m, \{v^e\}_{e=1}^m$. Further, searching over the space of DAGs is super-exponential in the number of variables. These computational challenges are common in causal structure learning problems and are made worse with the presence of multiple environments and hidden confounding. In this section, we propose some heuristics for computing *DirectLikelihood* based on perturbation data to find optimal scoring DAGs; we discuss open questions regarding computations involving the *DirectLikelihood* in Section 7.

The outline of this section is as follows: in Section 5.1, we describe a method to compute *DirectLikelihood* for a given DAG structure, that is, when the support of B is pre-specified. Building on this, in Section 5.2, we describe some computational heuristics for structure search over different DAGs.

5.1 Scoring a DAG

As announced above, we assume here that a DAG hence also the support of B are pre-specified. The goal is, for a given DAG, to estimate the unknown parameters. As prescribed in Section 2.1, we employ the *DirectLikelihood* procedure to fit the perturbation model where the hidden variables are independent and identically distributed across all the environments. In other words, we reparametrize (5) by setting $\Psi^e \rightarrow (1 + \psi^e) \mathcal{I}$. While the optimization program (5) is jointly non-convex, solving for the connectivity matrix B with the nuisance parameters ψ, Γ , and $\{w^e\}_{e=1}^m$ fixed is a convex program. Since we are mainly interested in an accurate estimate for the connectivity matrix, we propose the following alternating minimization strategy: starting with an initialization of all of the

model parameters, we fix B and perform gradient updates to find updated estimates for the nuisance parameters, and then update B – by solving a convex program to optimality with the remaining parameters fixed. We find that the alternating method described above is relatively robust to the initialization scheme, but we nonetheless propose the following concrete strategy:

$$\begin{aligned}
& 1) B_{(0)} \text{ via linear regression with observational data} \\
& 2) u_{(0)} = \text{diag} \left\{ \mathcal{I} - B_{(0)} \right\} \hat{\Sigma}^{-1} (\mathcal{I} - B_{(0)})^T \\
& 3) \Gamma_{(0)} = U D^{1/2} \text{ where } U D U^T \text{ is SVD of } (\mathcal{I} - B_{(0)}) \hat{\Sigma}^{-1} (\mathcal{I} - B_{(0)})^T - d_{(0)} \\
& 4) \text{ initialize } w_{(0)}^e = u_{(0)} + \zeta^e \mathbf{1} \text{ and solve } \zeta^e, \psi^e \text{ by 2-dimensional gridding,}
\end{aligned} \tag{15}$$

where the first step follows since the DAG structure is known, the fourth step is based on the observation that for a fixed B, Γ, u_0 , the optimization problems for ζ^e , and ψ^e decouples across the environments $e = 1, 2, 3, \dots, m$. The entire procedure, involving the initialization step and the parameter updates is presented in Algorithm 1.

Algorithm 1 Scoring \mathcal{D} via *DirectLikelihood*

- 1: **Input:** $\hat{\Sigma}^e$; $\text{do}(e)$ for $e = 1, 2, \dots, m$, regularization $\lambda \geq 0$
 - 2: **Initialize parameters:** via relation (15)
 - 3: **Alternating minimization:** Perform alternating iterates for positive integers t until convergence at iteration T :
 - (a) Fixing $(\Gamma_{(t)}, \{(\psi_{(t)}^e, w_{(t)}^e)\}_{e=1}^m)$, update $B_{(t+1)}$ by solving the convex optimization program (5). Fixing $B_{(t+1)}$, perform gradient updates until convergence to find $(\Gamma_{(t+1)}, \{(\psi_{(t+1)}^e, w_{(t+1)}^e)\}_{e=1}^m)$
 - (b) Perform alternating steps until convergence
 - 4: **Compute score $_{\lambda}(\mathcal{D})$:** plug-in the estimates $(B_{(T)}, \Gamma_{(T)}, \{(\psi_{(T)}^e, w_{(T)}^e)\}_{e=1}^m)$ into (6)
 - 5: **Output:** $\text{score}_{\lambda}(\mathcal{D})$ and the connectivity matrix $B_{(T)}$
-

Step 3 of Algorithm 1 involves two convergence criteria: the convergence of the gradient steps for the parameters $(\Gamma_{(t)}, \{(\psi_{(t)}^e, w_{(t)}^e)\}_{e=1}^m)$ as well as the convergence of the alternating procedure. For the first criterion, we terminate the gradient descent when the relative change in the likelihood score is below ϵ_1 . For the second criterion, we terminate the alternating minimization at step T when $\|B_{(T)} - B_{(T-1)}\|_{\infty} \leq \epsilon_2$. In the numerical experiments in Section 6, we set $\epsilon_1 = 10^{-7}$ and $\epsilon_2 = 10^{-3}$. Further, we set the learning rate in the gradient steps to be 0.001. Finally, for all our experiments, we set the regularization parameter λ to be twice the BIC analogue [20].

5.2 Identifying candidate DAGs

We have discussed how to score a given DAG using the *DirectLikelihood* estimator. Searching over all DAGs is typically not possible unless the number of observed variables p is small. In fact, performing a combinatorial search is known to be very challenging and in some sense NP-hard [6]. One could rely on greedy strategies [5]; we discuss below a strategy which exploits a reasonable set of candidate DAGs. In some applications with domain expertise, a set of plausible DAGs may be considered as candidate DAGs to be scored by the *DirectLikelihood*. Without this knowledge however, this candidate set must be obtained from data. In this section, we propose a heuristic to identify a collection of candidate DAGs to be score via Algorithm 1. Our approach is to identify these DAGs by assuming no hidden confounding. In general, fitting a DAG without taking into account the effect of hidden variables yields a denser graph (compared to the population or Markov equivalent DAGs) since marginalization of hidden variables induces confounding dependencies. As such, scoring such DAGs using Algorithm 1 may yield connectivity matrices that are more dense than the population connectivity matrix, although the magnitude of the spurious edges will be small. Thus, simply looking at the strongest edges or a crude thresholding of the entries of the connectivity matrices may compensate for the overly dense candidate DAGs, or one could also do some backward deletion from scored DAGs resulting to consider sub-DAGs of the candidate set.

In Section 1, we outlined procedures to identify DAGs without hidden confounding, with the constraint based PC algorithm, score based GES, and the hybrid method ARGES being among the most popular for structure learning in the observational setting. In principal, when domain expertise is not available, many of these methods can be used to find candidate DAGs. For simplicity, in our synthetic illustrations in Section 6, we perform GES on pooled environmental data. The GES procedure greedily adds or deletes edges in the space of Markov equivalent DAGs based on ℓ_0 regularized likelihood score and is asymptotically consistent [5]. We select the regularization parameter to be twice the analogue from the BIC score (as was suggested in [20]). Algorithm 2 presents the entire procedure of finding candidate DAGs, scoring them, and selecting the final output.

Algorithm 2 Optimizing *DirectLikelihood*

- 1: **Input:** $\hat{\Sigma}^e$; $\text{do}(e)$ for $e \in 1, 2, \dots, m$; regularization parameter $\lambda > 0$
 - 2: **Find candidate DAGs:** $\mathcal{D}_{\text{cand}} = \mathcal{D}_1, \mathcal{D}_2, \dots, \mathcal{D}_q$ using domain expertise, GES with pooled data, or some structure learning algorithm
 - 3: **Score each DAG:** For each \mathcal{D}_i , compute $\text{score}_\lambda(\mathcal{D}_i)$ and corresponding \hat{B}_i via Algorithm 1
 - 4: **Output:** Compute $\hat{\mathcal{D}}_{\text{opt}} = \arg \max_{\mathcal{D} \in \mathcal{D}_{\text{cand}}} \text{score}_\lambda(\mathcal{D})$ and the associated \hat{B}_{opt} . (Note that the arg max may not be unique in the infinite sample limit, due to potential non-identifiability. In practice, the optimization is done to find all optimal DAGs within a tolerance value from the minimum, and outputs also its several associated parameter estimates.
-

A few remarks regarding Algorithm 2 are in order. Since the scoring procedure in Algorithm 1 involves some heuristics and there may be multiple DAGs that yield an optimal score, one may more conservatively choose “near” optimal scoring DAGs in step 4 of Algorithm 2. Second, since the candidate DAGs $\mathcal{D}_{\text{cand}}$ may be overly dense due to the hidden effects, the optimal connectivity matrix \hat{B}_{opt} may consist of weak but nonzero spurious edges. In our numerical experiments in Section 6, we use the entries of \hat{B}_{opt} to rank the edges according to their absolute strengths. One may simply also threshold the edges at a pre-specified level.

6 Experiments

In this section, we illustrate the utility of *DirectLikelihood* with simulated and real data. In Section 6.1, we study the accuracy of the *DirectLikelihood* procedure in estimating the population causal graph underlying the observed variables. In Section 6.2, we provide comparisons of *DirectLikelihood* with the two-stage deconfounding procedure [11]. In Section 6.3, we examine *DirectLikelihood* under model miss-specifications, namely: non-Gaussian variables in a linear structure equation model, dependent latent variables, and non-linear SCMs. Finally in Section 6.4, we evaluate *DirectLikelihood* on the task of learning a causal network from a protein mass spectroscopy dataset [28].

Setup for synthetic experiments: we consider a collection of $p = 10$ observed variables influenced by $h \in \{1, 2\}$ hidden variables. To generate the connectivity matrix $B^* \in \mathbb{R}^{p \times p}$, we sample from an Erdős Rényi graph with edge probabilities 0.1 until we find a DAG structure, and form B^* by setting edge strengths equal to 0.7. The resulting DAG and connectivity matrix consists of 10 nonzero entries. The entries of the hidden coefficient matrix $\Gamma^* \in \mathbb{R}^{p \times h}$ are generated IID distributed uniformly from the interval $[0, \sqrt{2}]$ and the entries below $0.5\sqrt{2}$ are set to zero. The noise term ϵ is distributed according to $\epsilon \sim \mathcal{N}(0, 0.5\mathcal{I}_p)$. Unless otherwise specified, the hidden variables H are generated as $H \sim \mathcal{N}(0, \mathcal{I}_h)$. These parameters specify the distribution of the observed and hidden variables when there are no perturbations and we denote this environment by $e = 1$. In addition to this observational environment, we suppose there are $m - 1$ interventional environments. The number of samples generated in the observational environment is set to $n^1 = 300$ and $n^e = 5t$ for positive integer t . The values for t , the number of environments, and the magnitude of perturbations on the observed and hidden variables is specified later.

We compare the accuracy of the DAG structures of an estimated connectivity matrix and the population connectivity matrix as follows: a false positive is incurred if an edge produced in the estimated DAG is missing or is in the reverse direction in the population DAG. A true positive is achieved if an edge in the estimated DAG is present in the correct direction in the population DAG.

6.1 DAG structural recovery

We consider the synthetic setup described in Section 6. For each environment, we set $\delta_k^e \sim \mathcal{N}(0, \zeta + \text{Unif}(0, 1))$ for $k = 1, 2, \dots, p$ and certain values of ζ , and $H^e \sim (1 + \psi^e)\mathcal{N}(0, \mathcal{I}_h)$ with $\psi^{e,*} \sim \text{Unif}(0, 0.5)$. We generate data from $m = 7$ environments, one observational environment with no perturbations and six interventional environments, and consider the following five settings (a) $h = 1, \zeta = 5$, (b) $h = 1, \zeta = 2$, (c) $h = 2, \zeta = 5$, and (d) $h = 1, \zeta = 5$ and the last five environments have two observed variables that are chosen randomly to receive do-interventions with values set identically equal to 5. The perturbation data for each setting is supplied to the *DirectLikelihood* procedure to evaluate a score each DAG in a collection of candidate DAGs. We set $\bar{h} = h + 1$ in the *DirectLikelihood* estimator (5) and constrain the hidden variable perturbation $\psi^e \leq \psi_{\max} = 0.5$ for interventional environments $e = 2, 3, \dots, 7$. We then compute the accuracy of using the *DirectLikelihood* procedure (Algorithm 2) for DAG structural recovery in each of the settings (a – d) averaged across 10 independent trials. Fig 2 demonstrates these results when the candidate DAGs are obtained by performing the GES algorithm on pooled data. To ensure that the accuracy of our results is not simply due to the pooled GES, we compute the average size of the observational Markov equivalence class obtained after the pooled GES step in setting (a): 9 DAGs for $t = 64$, 8.8 for $t = 16$, 9.3 for $t = 4$, 6 for $t = 2$, 6.4 for $t = 1$.

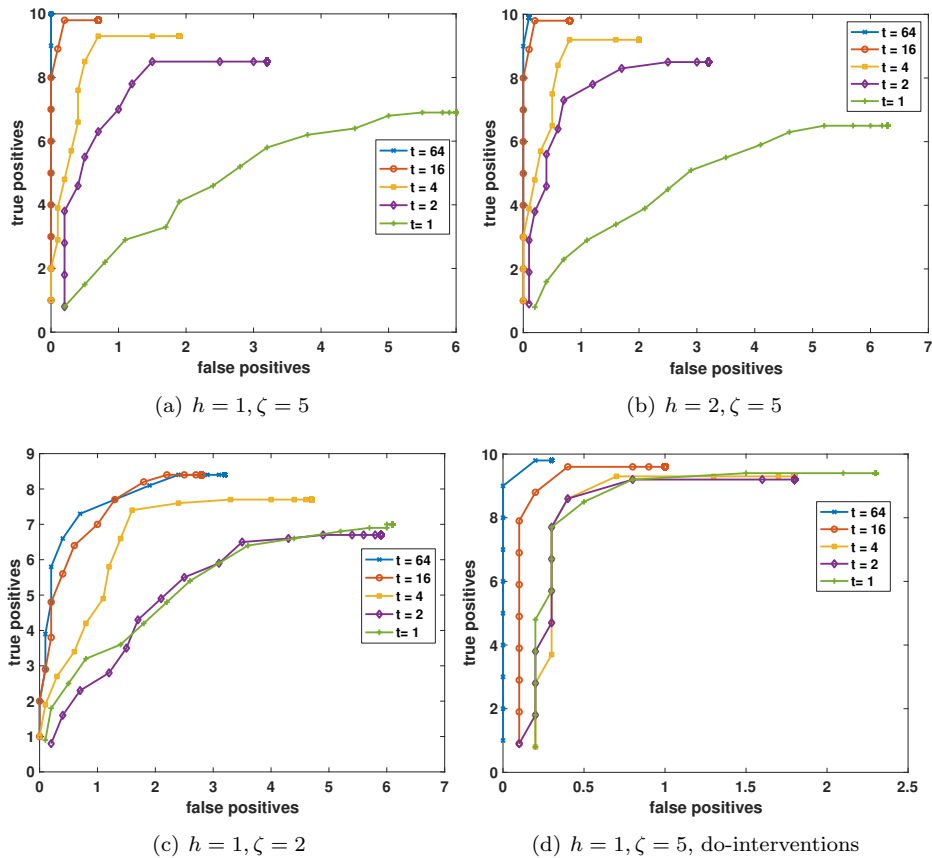


Figure 2: Structure estimation accuracy of Algorithm 2 (best scoring DAG) using candidate DAGs obtained by the GES algorithm on pooled data for different problem settings. Total number of true discoveries equals to 10. The curve for each t corresponds to $5t$ samples for each interventional environment, with $t \in \{1, 2, 4, 16, 64\}$. For each curve, the accuracy of the estimated DAG in comparison to the population DAG is calculated by ordering the edges according to their strengths and sequentially counting (from strongest edge to weakest edge) an edge to be a false discovery if it is missing or in a reverse direction in the population DAG, and otherwise count as a true discovery. Each curve is average across 10 independent trials.

6.2 Comparison to two-stage deconfounding and backShift

We compare the performance of *DirectLikelihood* to two methods: two-stage deconfounding and backShift. The two-stage deconfounding procedure first employs a sparse+low-rank decomposition on data from each environment

to deconfound the hidden variable effects and then employs the *DirectLikelihood* procedure with $\Gamma \equiv 0$ (i.e. no hidden affects) in the second stage. The two-stage deconfounding procedure for causal structure learning was introduced in [11] for observational setting and can be naturally extended to observational and interventional settings. As described in Section 1, the accuracy of the first step heavily relies on the denseness of the hidden variables. The backShift procedure introduced in [27] performs joint diagonalization of differences of covariance matrices; it is designed to identify cyclic graphs from interventional data (identifiability guarantees extend to acyclic graphs) under arbitrary number of hidden variables as long as the hidden variables remain unperturbed.

We generate the following synthetic example to compare the performance of these algorithms. We set $h = 3$ and consider the synthetic setup described earlier in this section with the following modifications: the columns of $\Gamma^* \in \mathbb{R}^{p \times 3}$ consist of a the standard basis elements with the coordinate corresponding to X_6 and X_5 nonzero, and a third column with entries sampled IID from the uniform distribution and the entries below 0.5 are set to zero. We generate an observational environment $e = 1$ and four interventional environments $e = 2, 3, 4, 5$ where $\delta_k^e \sim \mathcal{N}(0, \zeta + \text{Unif}(0, 1))$ for $k = 1, 2, \dots, p$ with $\zeta = 2$. We generate the hidden perturbation coefficient $\psi^e \sim \text{Uniform}(0, 0.5)$. We obtain $n^1 = 1000$ IID observational data and $5t$ IID interventional data for each interventional environment with $t \in \{20, 200\}$.

The *DirectLikelihood* procedure and two-stage deconfounding procedures both rely on choosing parameters that control the number of hidden variables (\bar{h} in *DirectLikelihood* and two regularization parameters in two-stage deconfounding procedure). Since we are interested in comparing identifiability properties of these procedures, we choose $\bar{h} = 3$ in *DirectLikelihood*. Further, we chose the regularization parameters in the deconfounding step of the two-stage deconfounding procedure as to optimize prediction while ensuring that the number of latent variables is less than or equal to 3. Specifically, we take 80% of the data (at random) as training samples, and the remaining 20% as test samples. After sweeping through the two regularization parameters, we choose the best performing model on the test set that have number of latent variables less than or equal to h . Both the *DirectLikelihood* procedure and the second stage two-stage deconfounding score a set of candidate DAGs. Noticing that the sparseness of the hidden effects induces a spurious edges between the pairs $(X_9, X_8), (X_{10}, X_9), (X_6, X_8)$, we generate the set of candidate DAGs by adding the directed edge $X_9 \rightarrow X_8, X_{10} \rightarrow X_9, X_6 \rightarrow X_8$ to the population DAG \mathcal{D}_X^* and consider 11 DAGs that add an additional edge at random. Further, we take the 8 members in the Markov equivalence class of the population DAG. Thus, the total number of candidate DAGs is equal to 20.

We consider the vanilla backShift output after thresholding the magnitude of the entries of the estimated connectivity matrix at 0.25. As prescribed in [27], we also consider the output after stability selection (with stability parameter 0.75) on top of the joint diagonalization algorithm to select stable edges.

Table 2 compares the structural recovery (across 10 independent trials) of *DirectLikelihood*, the two-stage deconfounding procedure, and backShift (with and without stability select). Evidently, the backShift procedure performs much more poorly than the other methods, which may be due to the perturbations on the hidden variables (not allowed for identifiability) as well as algorithmic instabilities that were also reported by the authors [27]. Next, we observe that since the denseness assumption is violated, the two-stage deconfounding produces a DAG with false positives, even when the number of samples in each environment is large (i.e. 1000 samples). Furthermore, in the low-sample regime, the two-stage procedure yields fewer true discoveries than *DirectLikelihood*. It is worth noting that in addition to the superior performance of *DirectLikelihood* as compared to two-stage deconfounding, the *DirectLikelihood* solution is faster to compute since it does not involve tuning two regularization parameters (as with two-stage deconfounding).

Method	$t = 10$	$t = 200$
<i>DirectLikelihood</i>	TP = 10, FP = 2.4	TP = 10, FP = 0
two-stage deconfounding	TP = 7.4, FP = 2.6	TP = 10, FP = 3
backShift	TP = 7.4, FP = 53.5	TP = 6.8, FP = 50.1
backShift with stability	TP = 0, FP = 0	TP = 0, FP = 0

Table 2: Comparison of *DirectLikelihood* with two-stage deconfounding and backShift procedures. Maximum possible number of true discoveries is equal 10. There are 1000 samples in the observational environment and $5t$ samples in each of the interventional environments.

6.3 Model miss-specification

We next explore the robustness of *DirectLikelihood* to model miss-specifications. We consider three types of model miss-specifications: non-Gaussian noise terms in the linear SCM (2) so that the observed variables are non-Gaussian, non-IID hidden variables, and non-linear functional forms in the SCM. We consider the synthetic setup described earlier where the data is generated with two hidden variables (i.e. $h = 2$) in the first two settings and with one hidden variable (i.e. $h = 1$) in the non-linear setting. Below we describe the specific modifications for each problem setting:

- Non-Gaussian: $\epsilon_k \sim \text{Unif}(-1, 1)$; $\delta_k^e \sim \text{Unif}(-5 + \text{Unif}(-1, 1), 5 + \text{Unif}(-1, 1))$ and $\psi^e \sim \text{Unif}(0, 0.2)$ for $k = 1, 2, \dots, p$ and $e = 2, 3, \dots, m$.
- Non-IID hidden variables: $\epsilon \sim \mathcal{N}(0, 0.5\mathcal{I}_p)$ and $H \sim \mathcal{N}\left(0, \begin{pmatrix} 1 & 0.2 \\ 0.2 & 1 \end{pmatrix}\right)$; $\delta_k^e \sim \mathcal{N}(0, 5 + \text{Unif}(0, 1))$ and $H^e \sim \mathcal{N}\left(0, \begin{pmatrix} 1 + \text{Unif}(0, 0.2) & 0.2 \\ 0.2 & 1 + \text{Unif}(0, 0.2) \end{pmatrix}\right)$ for $k = 1, 2, \dots, p$ and $e = 2, 3, \dots, m$.
- Non-linear SCM: $\epsilon \sim \mathcal{N}(0, 0.5\mathcal{I}_p)$ and $H \sim \mathcal{N}(0, 1)$; $\delta_k^e \sim \mathcal{N}(0, 5 + \text{Unif}(0, 1))$ and $H^e \sim (1 + \text{Unif}(0, 0.25))\mathcal{N}(0, 1)$ for every $k = 1, 2, \dots, p$ and $e = 2, 3, \dots, m$. Further, for every $k = 1, 2, \dots, p$: $X_k^e = B_{k, \text{pa}(k)}^* X_{\text{pa}(k)}^e + \gamma_k^T H^e + \xi \tanh(B_{k, \text{pa}(k)}^* X_{\text{pa}(k)}^e + \gamma_k^T H^e) + \epsilon_k + \delta_k^e$. We consider $\xi = \{0.3, 1\}$.

For each setting, we obtain data for an observational environment and 6 interventional environments, for a total of $m = 7$ environments. We supply the perturbation data to the *DirectLikelihood* procedure with $\bar{h} = 3$ and the constraint $\psi^e \leq \psi_{\max} = 0.5$ for the first two settings and $\bar{h} = 1$ and the constraint $\psi^e \leq \psi_{\max} = 0.5$ in the non-linear setting. For all problem instances, the set of candidate DAGs are obtained by employing GES on the pooled data. Fig 3 demonstrates the robustness of *DirectLikelihood* procedure to these model miss-specifications. We observe that the *DirectLikelihood* procedure provides an accurate estimate under non-Gaussian and non-IID hidden variable settings. Further, our method appears to be robust to some amount of non-linearity. We remark that the empirical success in the non-Gaussian setting is supported by our theoretical results in Section 3. As also noted in Section 3, our theoretical results can be extended to the setting with non-IID hidden variables. However, we are unable to provide any guarantees for non-linear SCMs.

6.4 Real experiment with protein expression dataset

We evaluate our algorithm on the task of learning a causal network from a protein mass spectroscopy dataset [28]. This data set contains a large number of measurements of the abundance of 11 phosphoproteins and phospholipids recorded under different experimental conditions in primary human immune system cells. The different experimental conditions are characterized by associated reagents that inhibit or activate signaling nodes, corresponding to interventions at different points of the protein-signaling network. Following the previous works [18, 17], we take 8 environments consisting of an observational environment and 7 interventional environments. Knowledge about some of the “ground truth” is available, which helps verification of results.

To identify a set of candidate DAGs to score using our *DirectLikelihood* procedure, we consider all DAGs that are Markov equivalent to the ground truth DAG reported in [28] (total of 176 DAGs) as well as the Markov equivalence class of the DAG reported in [18] (22 DAGs). We leave one interventional environment out and supply the data to *DirectLikelihood* estimator with $\bar{h} = 1$. We find the best scoring connectivity matrix and hidden variable coefficient matrix. We repeat this process by varying the interventional environment that is left out. Among the seven optimal connectivity matrices (across the seven settings), we keep the edges that appear at least five times, and compute the average strength of those edges. Fig 4 and Table 3 demonstrate the estimated graph and edge strengths, respectively. Further, we examine the effect of the estimated hidden variable on the proteins. Specifically, following [30], we compute the top singular vector of the average projection matrix (computed across the seven settings) onto the 1-dimensional hidden variable subspace. The magnitude of the entries of this singular vector are below 0.015 for all proteins except PKC, P38, and JNK, whose magnitudes are all above 0.5. Thus, we observe that the majority of the influence of the hidden variables appears to be on the proteins PKC, P38, and JNK.

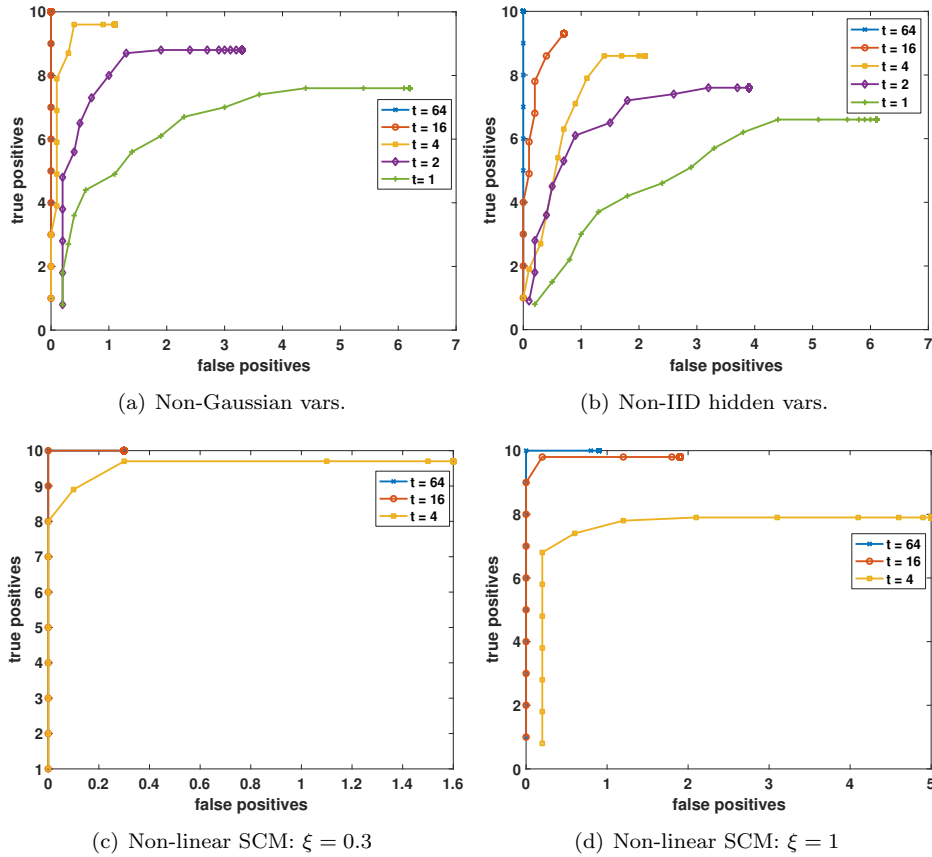


Figure 3: Robustness of DirectLikelihood under model misspecifications including non-Gaussian data, non-IID hidden variables, and non-linear SCM with different amounts of non-linearity. The total number of possible true discoveries equals 10. We consider $t \in \{1, 2, 4, 16, 64\}$ in the non-Gaussian and non-IID hidden settings and $t \in \{4, 16, 64\}$ in the non-linear SCM settings. In some problem settings, $t = 64$ has the same behavior as $t = 16$ and thus cannot be seen. The accuracy of the estimated DAGs via DirectLikelihood is evaluated in a similar fashion as Figure 2.

Finally, we compare our findings to the direct causal relations reported in the literature [10, 17, 18, 28] in Table 4. We observe that many of the strong edges reported by *DirectLikelihood* agree with the previous methods with the exception of the edges: $\text{Akt} \rightarrow \text{PKA}$ and $\text{Erk} \rightarrow \text{Mek}$.

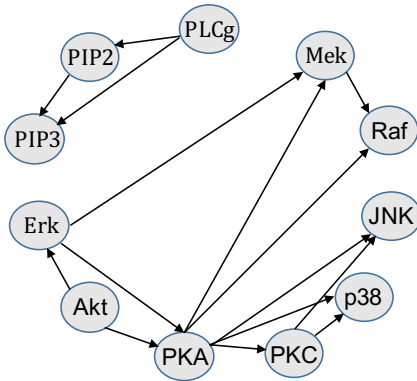


Figure 4: Estimated DAG by DirectLikelihood.

Edge	Average strength
PKC \rightarrow p38	1.71
Mek \rightarrow Raf	0.88
Akt \rightarrow Erk	0.67
PKC \rightarrow JNK	0.57
Akt \rightarrow PKA	0.26
PIP2 \rightarrow PIP3	0.22
PLCg \rightarrow PIP2	0.20
PLCg \rightarrow PIP3	0.14
Erk \rightarrow PKA	0.12
PKA \rightarrow P38	0.04
PKA \rightarrow PKC	0.03
PKA \rightarrow JNK	0.02
Erk \rightarrow Mek	0.01
PKA \rightarrow Mek	0.004
PKA \rightarrow Raf	0.001

Table 3: Average edge strengths obtained by DirectLikelihood.

Edge	[28](a)	[28](b)	[18]	[10]	[17]
PKC → p38	✓	✓	✓	✓	✓
Mek → Raf			✓	✓	✓
Akt → Erk			✓		✓
PKC → JNK	✓	✓	✓	✓	
Akt → PKA					
PIP2 → PIP3			✓		
PLCg → PIP2	✓	✓		✓	✓
PLCg → PIP3		✓		✓	
Erk → PKA				✓	
PKA → P38	✓	✓	✓		
PKA → PKC				✓	
PKA → JNK	✓	✓	✓	✓	
Erk → Mek					
PKA → Mek	✓	✓	✓	✓	
PKA → Raf	✓	✓			

Table 4: Comparing the findings of *DirectLikelihood* (ordered by edge strength) with different causal discovery methods. Here, we are only including edges found by *DirectLikelihood* and note that additional edges have been identified by the other methods. The consensus network according to [28] is denoted by “[28](a)” and their reconstructed network by “[28](b)”.

7 Discussion

In this paper, we proposed a framework to model perturbation data among a collection of Gaussian observed and hidden variables. It can be represented as a certain mixed-effects linear structural causal model where the interventions are modeled as random effects which propagate dynamically through the structural equations. This framework allows for perturbations on all components of the system, including a target variable of interest or the hidden variables. In contrast to previous techniques that do not allow for such perturbations, our maximum-likelihood estimator *DirectLikelihood* identifies the population DAG structure among the observed variables under relatively mild assumptions. The most restrictive assumption (dubbed *hidden spuriousness*) requires that the hidden variables induce some confounding among the observed variables, and is far less stringent than hidden denseness assumption that is needed for the two-stage deconfounding procedure [11]. We further specialized the theoretical guarantees to the setting where the hidden variables are unperturbed or when there are no hidden affects. Finally, we demonstrated the utility of *DirectLikelihood* for identifying causal relationships on synthetic and real data.

There are several interesting directions for further investigation that arise from our work that we outline below:

Computational tools for DirectLikelihood : In Section 5, we proposed heuristics for searching over the space of DAGs and for solving the *DirectLikelihood* estimator (5) to score DAGs. While the empirical results in Section 6 support the utility of our heuristics, there is much room for more rigorous optimization techniques. Greedy approaches, for example, are common for causal structural identification and are sometimes supported by theoretical guarantees (e.g. GES [5]). A conceptual challenge with developing greedy-based techniques for *DirectLikelihood* is that the likelihood score is not decomposable according to the DAG structure due to the hidden confounding. One potential approach to overcome this challenge is to extend the sparsest poset framework developed in [2] to incorporate data from multiple environments.

High-dimensional consistency analysis of DirectLikelihood : The theoretical results in Section 3 are based on analysis in the large data limit. However, our empirical results in Section 6 suggest that the *DirectLikelihood* procedure may provide accurate estimates with moderate data size. As such, an exciting research direction is to develop high-dimensional consistency guarantees for *DirectLikelihood*. A possible approach is to extend the results of [31] in the context of causal learning from observational data to the setting where there are multiple environments and hidden confounding.

Characterizing the interventional Markov equivalence class: In the setting where the perturbations are limited, there may be multiple DAGs that are equally representative of the data, or equivalently, multiple DAGs that yield the same exact likelihood score in the population case.. The class of equally scoring DAGs forms an equivalence

class, and is known as the Markov equivalence class in the observational setting, and as interventional Markov equivalence class in the setting with perturbed data. The characterization of these equivalence classes was central to developing structural learning algorithms [5, 12] as well as constructing active learning strategies for maximally informative interventions [13]. Obtaining an understanding of the interventional Markov equivalence class for our problem may enable similar consequences.

Beyond linear models: The perturbation model (2) assumes a linear relationship between the observed and hidden variables. In certain applications, the linearity assumption may be restrictive, necessitating a richer model class to capture the underlying causal relations. The conceptual leap to non-linearity was considered in [15] by extending the Invariant Causal Prediction (ICP) methodology to non-linear models. As with the ICP technology, [15] assumes that there are no hidden confounders and that the target variable remains unperturbed. Given that our framework overcame these challenges in the linear setting, it would be of interest to explore extensions to the non-linear setting. Alternatively, one can characterize the extent to which linear models capture the causal effects [7].

Acknowledgements

A. Taeb and P. Bühlmann have received funding from the European Research Council under the Grant Agreement No 786461 (CausalStats - ERC-2017-ADG). They both acknowledge scientific interaction and exchange at “ETH Foundations of Data Science”. The authors would like to thank Mona Azadkia, Yuansi Chen and Juan Gamella for helpful discussions and feedback on the manuscript.

References

- [1] J. ANGRIST, G. IMBENS, AND D. RUBIN, *Identification of causal effects using instrumental variables*, Journal of the American Statistical Association, 91 (1996), pp. 444–455.
- [2] D. BERNSTEIN, B. SAEED, C. SQUIRES, AND C. UHLER, *Ordering-based causal structure learning in the presence of latent variables*, International Conference on Artificial Intelligence and Statistics, (2020), pp. 4098–4108.
- [3] P. BÜHLMANN, *Invariance, causality and robustness*, Statistical Science, 35 (2020), pp. 404–426.
- [4] V. CHANDRASEKARAN, P. PARILLO, AND A. WILLSKY, *Latent variable graphical model selection via convex optimization*, Annals of Statistics, 40 (2012), pp. 1935–1967.
- [5] D. CHICKERING, *Optimal structure identification with greedy search*, Journal of Machine Learning Research, 3 (2002), pp. 507–554.
- [6] D. CHICKERING, C. MEEK, AND D. HECKERMAN, *Large-sample learning of bayesian networks is np-hard*, Journal of Machine Learning Research, 5 (2004), pp. 1287–1330.
- [7] R. CHRISTIANSEN, N. PFISTER, M. JAKOBSEN, AND N. GNECCO, *The difficult task of distribution generalization in nonlinear models*, arXiv:2006.07433, (2020).
- [8] A. DIXIT, O. PARNAS, AND B. LI, *Perturb-seq: dissecting molecular circuits with scalable single-cell rna profiling of pooled genetic screens*, Cell, 167 (2016), pp. 1853–1866.
- [9] M. DRTON AND M. MAATHIUS, *Structure learning in graphical modeling*, Annual Review of Statistics and Its Application, 4 (2017), pp. 365–393.
- [10] D. EATON AND K. MURPHY, *Exact bayesian structure learning from uncertain interventions*, In Proceedings of the 10th International Conference on Artificial Intelligence and Statistics (AISTATS), (2007).
- [11] B. FROT, P. NANDY, AND M. MAATHIUS, *Robust causal structure learning with hidden variables*, Journal of Royal Statistical Society, Series B, 81 (2019), pp. 459–487.
- [12] A. HAUSER AND P. BÜHLMANN, *Characterization and greedy learning of interventional markov equivalence classes of directed acyclic graphs*, Journal of Machine Learning Research, 13 (2012), pp. 2409–2464.

- [13] A. HAUSER AND P. BÜHLMANN, *Two optimal strategies for active learning of causal models from interventional data*, International Journal of Approximate Reasoning, 4 (2014), pp. 926–939.
- [14] A. HAUSER AND P. BÜHLMANN, *Jointly interventional and observational data: estimation of interventional markov equivalence classes of directed acyclic graphs*, Journal of Royal Statistical Society, Series B, 77 (2015), pp. 291–318.
- [15] C. HEINZE-DEMLE, J. PETERS, AND N. MEINSHAUSEN, *Invariant causal prediction for nonlinear models*, Journal of Causal Inference, 6 (2018), pp. 1–35.
- [16] A. MCLEAN, L. SANDERS, AND W. WALTER, *A unified approach to mixed linear models*, Journal of American Statistical Association, 45 (1991), pp. 54–64.
- [17] N. MEINSHAUSEN, A. HAUSER, J. MOOIJ, J. PETERS, P. VERSTEEG, AND P. BÜHLMANN, *Methods for causal inference from gene perturbation experiments and validation*, Proceeding of National Academy of Sciences, 113 (2016), pp. 7361–7368.
- [18] J. MOOIJ AND T. HESKES, *Cyclic causal discovery from continuous equilibrium data*, In Proceedings of the 29th Annual Conference on Uncertainty in Artificial Intelligence, (2013), pp. 431–439.
- [19] P. NANDY, A. HAUSER, AND M. MAATHIUS, *High-dimensional consistency in score-based and hybrid structure learning*, Annals of Statistics, 46 (2018), pp. 3151–3183.
- [20] C. NOWZOHOUR AND P. BÜHLMANN, *Score-based causal learning in additive noise models*, Statistics, 50 (2016), pp. 471–485.
- [21] J. PEARL, *Causality: Models, reasoning, and inference*, Cambridge University Press, 2nd edition, 2009.
- [22] J. PETERS AND P. BÜHLMANN, *Identifiability of gaussian structural equation models with equal error variances*, Biometrika, 101 (2014), pp. 219–228.
- [23] J. PETERS, P. BÜHLMANN, AND N. MEINSHAUSEN, *Causal inference using invariant prediction: identification and confidence intervals*, Journal of the Royal Statistical Society, Series B, 78 (2016), pp. 947–1012.
- [24] J. ROBINS, M. HERNAN, AND B. BRUMBACK, *Marginal structural models and causal inference in epidemiology*, Epidemiology, 11 (2000), pp. 550–560.
- [25] D. ROTHENHÄUSLER, P. BÜHLMANN, AND N. MEINSHAUSEN, *Causal dantzig: fast inference in linear structural equation models with hidden variables under additive interventions*, Annals of Statistics, 47 (2019), pp. 1688–1722.
- [26] D. ROTHENHÄUSLER, N. MEINSHAUSEN, P. BÜHLMANN, AND J. PETERS, *Anchor regression: heterogeneous data meets causality*, arXiv:1801.06229, (2020).
- [27] D. ROTHENHÄUSLER, C. HEINZE, J. PETERS, AND N. MEINSHAUSEN, *backshift: Learning causal cyclic graphs from unknown shift interventions*, In Advances in Neural Information Processing Systems, (2016).
- [28] K. SACHS, O. PEREZ, D. LAUFFENBURGER, AND G. NOLAN, *Causal protein-signaling networks derived from multiparameter single-cell data*, Science, 308 (2005), pp. 523–529.
- [29] P. SPIRITES, C. GLYMOUR, AND R. SCHEINES, *Causation, Prediction, and Search*, Cambridge: MITPress, 2000.
- [30] A. TAEB, P. SHAH, AND V. CHANDRASEKARAN, *False discovery and its control in low-rank estimation*, Journal of Royal Statistical Society, Series B, 82 (2020), pp. 992–1027.
- [31] S. VAN DE GEER AND P. BÜHLMANN, *ℓ_0 -penalized maximum likelihood for sparse directed acyclic graphs*, Annals of Statistics, 41 (2013), pp. 536–567.
- [32] T. VERMA AND J. PEARL, *Equivalence and synthesis of causal models*, In Proceedings of the 6th Conference on Uncertainty in Artificial Intelligence (UAI), (1991), pp. 255–270.
- [33] Y. WANG, L. SOLUS, K. YANG, AND C. UHLER, *Permutation based causal inference algorithms with interventions*, In Advances in Neural Information Processing Systems, (2017), pp. 5822–5831.

A Supplementary Material

The proof of the theoretical results are based on the following population quantities that we summarize. Let $B^* \in \mathbb{R}^{p \times p}$ be the population connectivity matrix, $\Gamma^* \in \mathbb{R}^{p \times h}$ be the hidden coefficient matrix, $w^{1,*} \in \mathbb{R}_{++}^p$ encode the variance of the coordinates of ϵ , $\text{diag}(w^{e,*}) \in \mathbb{S}_+^p$ be a non-negative diagonal matrix encoding the perturbations on the observed variables, $w^{e,*} \in \mathbb{R}_{++}^p$ with $w_k^{e,*} = w_k^{1,*} + w_k^{e,*}$. Let $\{\psi^{e,*}\}_{e=1}^m \subset \mathbb{R}_+$ be the perturbation on the hidden variables. Let $\kappa^* = \frac{1 + \max_i \|B_{:,i}^*\|_2}{1 + \min_i \|B_{:,i}^*\|_2}$. Finally, for a matrix $M \in \mathbb{R}^{d \times d}$, we denote $\|M\|_2$ as the spectral norm (largest singular value) of M .

A.1 Proof of Theorem 1

For notational convenience, we restate the *DirectLikelihood* estimator (5) in the presence of perturbed IID hidden variables and observational data

$$\begin{aligned} (\hat{B}, \hat{\Gamma}, \hat{\psi}, \{\hat{w}^e\}_{e=1}^m) = & \arg \min_{B, \Gamma, \psi \in \mathbb{R}_+^m, \{w^e\}_{e=1}^m \subseteq \mathbb{R}_{++}^p} \sum_{e=1}^m \pi^{e,*} \ell(B, \Gamma, (1 + \psi^e)\mathcal{I}, w^e) \\ & \text{subject-to. } B \text{ compatible with } \mathcal{D} ; \|\psi\|_\infty \leq C_\psi \\ & \psi^1 = 0 ; w^e \succ w^1 \text{ for } e = 2, \dots, m \end{aligned} \quad (16)$$

with a score function defined as in (6) with $\lambda = 0$. Here the decision variable ψ encodes the latent perturbations and consists of coordinates $\psi = (\psi^e, \psi^2, \dots, \psi^m)$. The optimal DAG is given by $\mathcal{D}_{\text{opt}} = \min_{\mathcal{D}} \text{score}_{\lambda=0}(\mathcal{D})$ with associated connectivity matrices B_{opt} .

The proof strategy for proving Theorem 1 is based on appealing to the following three lemmas:

Lemma 1. *Optimal solutions of (16) satisfy the following equivalence:*

$$\begin{aligned} (B, \Gamma, \psi, \{v^e\}_{e=1}^m) \text{ optimum of (16)} \\ \iff B \text{ is DAG, } \|\psi\|_\infty < C_\psi, \psi^1 = 0 \ \& \ \text{for every } e = 1, 2, \dots, m \\ \Sigma^{e,*} = (\mathcal{I} - \mathcal{F}_{\text{do}(e)^c} B)^{-1} (\text{diag}(w^e) + (\psi^e + 1)[\Gamma \Gamma^T]_{\text{do}(e)^c}) (\mathcal{I} - \mathcal{F}_{\text{do}(e)^c} B)^{-T}. \end{aligned}$$

Lemma 2. *Let $(\tilde{B}, \tilde{\Gamma}, \tilde{\psi}, \{\tilde{w}^e\}_{e=1}^m)$ be an optimal solution of (16). The following statements hold:*

1. *Suppose $\tilde{\psi}^e \neq \psi^{e,*}$ for some $e \in \{2, 3\}$. Under Assumptions 1-5 in (10) or Assumptions 6-10 in (11), $\text{moral}(B^*) \subset \text{moral}(\tilde{B})$.*
2. *Suppose $\tilde{\psi}^e = \psi^{e,*}$ for $e = 2, 3$. Under Assumptions 1-5 in (10) or Assumptions 6-10 in (11), $\text{moral}(\tilde{B}) = \text{moral}(B^*)$.*

Lemma 3. *Let $(\tilde{B}, \tilde{\Gamma}, \tilde{\psi}, \{\tilde{w}^e\}_{e=1}^m)$ be an optimal solution of (16). Suppose $\tilde{\psi}^e = \psi^{e,*}$ for $e = 2, 3$. Then, $\tilde{B} = B^*$.*

Combining Lemma 2 and 3 will conclude the proof of Theorem 1, due to the fact that the true parameter values leads to an optimum of (16). We now prove each lemma.

A.1.1 Useful notations

We introduce some notations that will be repeatedly used. Specifically, we define for $e \in \mathcal{E}$ where there are no do-interventions:

$$\begin{aligned} \kappa_{\text{cond}}^e &\equiv \min_{k,l} |(\mathcal{I} - B^*)^T \text{diag}(w^{e,*})^{-1} (\mathcal{I} - B^*)|_{k,l} \\ &\text{s.t. } \rho(X_k^e, X_l^e | X_{\setminus\{k,l\}}^e, H^e) \neq 0 \\ \kappa_{\text{hidden}}^e &\equiv \max_{k,l} |(\mathcal{I} - B^*)^T \text{diag}(w^{e,*})^{-1} (\Gamma^{*T} \text{diag}(w^{e,*})^{-1} \Gamma^* + \frac{1}{1 + \psi^{e,*}} \mathcal{I})^{-1} \\ &\quad \text{diag}(w^{e,*})^{-1} (\mathcal{I} - B^*)|_{k,l} \\ &\text{s.t. } \rho(X_k^e, X_l^e | X_{\setminus\{k,l\}}^e, H^e) = 0 \end{aligned}$$

The intuition behind the quantities κ_{cond}^e and κ_{hidden}^e is based on the decomposition of $(\Sigma^{e,*})^{-1}$. Specifically, from the Woodbury inversion lemma:

$$\begin{aligned} (\Sigma^{e,*})^{-1} &= (\mathcal{I} - B^*)^T \text{diag}(w^{e,*})^{-1} (\mathcal{I} - B^*) \\ &\quad - (\mathcal{I} - B^*)^T \text{diag}(w^{e,*})^{-1} (\Gamma^{*T} \text{diag}(w^{e,*})^{-1} \Gamma^* + \frac{1}{1 + \psi^{e,*}} \mathcal{I})^{-1} \text{diag}(w^{e,*})^{-1} (\mathcal{I} - B^*) \end{aligned}$$

Standard multivariate analysis states that for any pair of indices (k, l) with $k \neq l$, $[(\Sigma^{e,*})^{-1}]_{k,l} \neq 0$ if and only if $\rho(X_k^e, X_l^e | X_{\setminus\{k,l\}}^e) \neq 0$. Similarly, since the precision matrix $\text{cov}(X^e | H^e)^{-1} = (\mathcal{I} - B^*)^T \text{diag}(w^{e,*})^{-1} (\mathcal{I} - B^*)$, we have that $[(\mathcal{I} - B^*)^T \text{diag}(w^{e,*})^{-1} (\mathcal{I} - B^*)]_{k,l} \neq 0$ if and only if $\rho(X_k^e, X_l^e | X_{\setminus\{k,l\}}^e, H^e) \neq 0$. Thus, by definition, $\kappa_{\text{cond}}^e > 0$ and by the *hidden spuriousness* in Definition 1, $\kappa_{\text{hidden}}^e > 0$. Then,

$$\kappa_{\text{cond}}^e \geq \frac{(1 + \min_i \|B_{:,i}^*\|_2^2)}{2 \max_k w_k^{e,*}}. \quad (17)$$

Similarly, we have due to $\min_k w_k^{e,*} \geq 8 \|\Gamma^*\|_2^2 (1 + C_\psi)$ and $\min_k w_k^{e,*} \geq 8 \|w^{1,*}\|_\infty$:

$$\kappa_{\text{hidden}}^e \geq \frac{8^3 (1 + \min_i \|B_{:,i}^*\|_2^2) (1 + \psi^{e,*})}{9^3 (\max_k w_k^{e,*})^2}. \quad (18)$$

A.1.2 Proof of Lemma 1

Proof. Let $\mathcal{M}(B, \Gamma, \psi^e, w^e)$ denote a model associated with each equation in the SCM (2). For notational convenience, we use the short-hand notation \mathcal{M}^e for this model. We let $\Sigma(\mathcal{M}^e) = (\mathcal{I} - \mathcal{F}_{\text{do}(e)^c} B)^{-1} (\text{diag}(w^e) + (1 + \psi^e) [\Gamma \Gamma^T]_{\text{do}(e)^c}) (\mathcal{I} - \mathcal{F}_{\text{do}(e)^c} B)^{-T}$ be the associated covariance model parameterized by the parameters (B, Γ, ψ^e, w^e) . The optimal solution of the population *DirectLikelihood* can be equivalently reformulated as:

$$\arg \min_{\{\mathcal{M}^e\}_{e=1}^m} \sum_{e=1}^m \pi^{e,*} \text{KL}(\Sigma^{*,e}, \Sigma(\mathcal{M}^e)). \quad (19)$$

Notice that for the decision variables $\mathcal{M}^{e,*} = (B^*, \Gamma^*, \psi^{e,*}, w^{e,*})$ for each $e = 1, 2, \dots, m$, (19) achieves zero loss. Hence, any other optimal solution of (19) must yield zero loss, or equivalently, $\Sigma(\mathcal{M}^e) = \Sigma^{e,*}$ for any optimal collection $\{\mathcal{M}^e\}_{e=1}^m$. \square

A.1.3 Proof of Lemma 2

Proof. We first provide the proof of Lemma 2 under Assumptions 1-5 in (10). Since there are no do-interventions in the environments $e = 1, 2, 3$ (according to Assumption 1), Lemma 1 implies that for every $e = 2, 3$,

$$\begin{aligned} &\Sigma^{e,*} - (1 + \tilde{\psi}^e) \Sigma^{1,*} \\ &= (\mathcal{I} - B^*)^{-1} \left(\text{diag} \left(w^{e,*} - (1 + \tilde{\psi}^e) w^{1,*} \right) + (\psi^{e,*} - \tilde{\psi}^e) \Gamma^* \Gamma^{*T} \right) (\mathcal{I} - B^*)^{-T} \\ &= (\mathcal{I} - \tilde{B})^{-1} \text{diag} \left(\tilde{w}^e - (1 + \tilde{\psi}^e) \tilde{w}^1 \right) (\mathcal{I} - \tilde{B})^{-T} \end{aligned} \quad (20)$$

Since $\min_k w_k^{e,*} \geq C_\psi (\|w^{1,*}\|_\infty + C_\psi \|\Gamma^*\|_2^2)$ from Assumption 3 in (10), we conclude that the matrix $\Sigma^{e,*} - (1 + \tilde{\psi}^e) \Sigma^{1,*}$ is invertible for $e = 2, 3$.

To establish the first component of Lemma 2, consider $e \in \{2, 3\}$ for which $\psi^{e,*} \neq \tilde{\psi}^e$. After an inversion of (20) for this environment, we obtain:

$$\begin{aligned} &(\mathcal{I} - B^*)^T (M^e + L^e) (\mathcal{I} - B^*) \\ &= (\mathcal{I} - \tilde{B})^T \text{diag} \left(\tilde{w}^e - (1 + \tilde{\psi}^e) \tilde{w}^1 \right)^{-1} (\mathcal{I} - \tilde{B}) \end{aligned} \quad (21)$$

where,

$$M^e = \text{diag} \left(w^{e,*} - (1 + \tilde{\psi}^e) w^{1,*} \right)^{-1} ; \quad L^e = M^e \Gamma^* \left[\Gamma^{*T} M^e \Gamma^* + \frac{1}{\Delta \psi^e} \mathcal{I} \right]^{-1} \Gamma^{*T} M^e,$$

Here, we have introduced a short-hand notation: $\Delta\psi^e = (\psi^{e,\star} - \tilde{\psi}^e)$. Notice that the nonzero entries of $(\mathcal{I} - \tilde{B})^T \text{diag}(\tilde{w}^e - (1 + \tilde{\psi}^e)\tilde{w}^1)^{-1} (\mathcal{I} - \tilde{B})$ encode the moral graph induced by \tilde{B} . Our strategy is to use Assumptions 1-5 in (10) to show $(\mathcal{I} - B^\star)^T(M^e + L^e)(\mathcal{I} - B^\star)$ has non-zeros in the entries corresponding to the moral graph of B^\star and at least one nonzero outside of the moral graph. To conclude this, we consider the following intermediate terms close to M^e and L^e :

$$\bar{M}^e = \text{diag}(w^{e,\star})^{-1} ; \bar{L}^e = \bar{M}^e \Gamma^\star \left[\Gamma^{\star T} \bar{M}^e \Gamma^\star + \frac{1}{1 + \psi^{e,\star}} \mathcal{I} \right]^{-1} \Gamma^{\star T} \bar{M}^e$$

Notice that:

$$\|\bar{M}^e - M^e\|_2 \leq \frac{5(1 + C_\psi)\|w^{1,\star}\|_\infty}{4(\min_k w_k^{e,\star})^2} ; \|M^e\|_2 \leq \frac{5}{4(\min_k w_k^{e,\star})} \quad (22)$$

where the inequalities follow by noting that $5(1 + C_\psi)\|w^{1,\star}\|_\infty \leq \min_k w_k^{e,\star}$ from Assumption 5 in (10). Now let (k, l) be any pair of indices connected in the moral graph of B^\star . Then:

$$\begin{aligned} |(\mathcal{I} - B^\star)^T M^e (\mathcal{I} - B^\star)|_{k,l} &\geq |(\mathcal{I} - B^\star)^T \bar{M}^e (\mathcal{I} - B^\star)|_{k,l} \\ &\quad - (1 + \max_i \|B_{:,i}^\star\|_2)^2 \|\bar{M}^e - M^e\|_2 \\ &\geq \kappa_{\text{cond}}^e - \frac{5(1 + C_\psi)\|w^{1,\star}\|_\infty (1 + \max_i \|B_{:,i}^\star\|_2^2)}{4(\min_k w_k^{e,\star})^2} \\ &\geq \frac{(1 + \min_i \|B_{:,i}^\star\|_2)^2}{2(\max_k w_k^{e,\star})} - \frac{5(1 + C_\psi)\|w^{1,\star}\|_\infty (1 + \max_i \|B_{:,i}^\star\|_2^2)}{4(\min_k w_k^{e,\star})^2} \\ &\geq \frac{(1 + \max_i \|B_{:,i}^\star\|_2^2)}{4 \max_k w_k^{e,\star}}. \end{aligned} \quad (23)$$

Here, the second to last inequality follows from the relation (17) and the last inequality follows from $\frac{\min_k w_k^{e,\star}}{\text{cond}(\text{diag}(w^{e,\star}))} \geq 5\kappa^\star(1 + C_\psi)\|w^{1,\star}\|_\infty$. Next, we control $\|(\mathcal{I} - B^\star)^T L^e (\mathcal{I} - B^\star)\|_\infty$. Using the inequality $\left[\Gamma^{\star T} M^e \Gamma^\star + \frac{1}{\Delta\psi^e} \mathcal{I} \right]^{-1} \preceq (\Delta\psi^e) \mathcal{I}$, we have that:

$$\|(\mathcal{I} - B^\star)^T L^e (\mathcal{I} - B^\star)\|_\infty \leq \frac{25C_\psi(1 + \max_i \|B_{:,i}^\star\|_2^2)\|\Gamma^\star\|_2^2}{16(\min_k w_k^{e,\star})^2} \quad (24)$$

Since $\frac{\min_k w_k^{e,\star}}{\text{cond}(\text{diag}(w^{e,\star}))} \geq 7C_\psi\|\Gamma^\star\|_2^2$, comparing (24) and (23), we conclude that for any indices (k, l) connected in the moral graph of B^\star

$$|(\mathcal{I} - B^\star)^T M^e (\mathcal{I} - B^\star)|_{k,l} > \|(\mathcal{I} - B^\star)^T L^e (\mathcal{I} - B^\star)\|_\infty.$$

To finish the proof of the first assertion of Lemma 2, we have to show that for indices (k, l) attaining the optimum κ_{hidden} , $|(\mathcal{I} - B^\star)^T L^e (\mathcal{I} - B^\star)|_{k,l} > 0$ or equivalently, $|(\mathcal{I} - B^\star)^T (\frac{1 + \psi^{e,\star}}{\Delta\psi^e} L^e) (\mathcal{I} - B^\star)|_{k,l} > 0$. Notice that:

$$\begin{aligned} \left| (\mathcal{I} - B^\star)^T \left(\frac{1 + \psi^{e,\star}}{\Delta\psi^e} L^e \right) (\mathcal{I} - B^\star) \right|_{k,l} &\geq |(\mathcal{I} - B^\star)^T \bar{L}^e (\mathcal{I} - B^\star)|_{k,l} \\ &\quad - |(\mathcal{I} - B^\star)^T \left(\frac{1 + \psi^{e,\star}}{\Delta\psi^e} L^e - \bar{L}^e \right) (\mathcal{I} - B^\star)|_{k,l} \\ &\geq \kappa_{\text{hidden}} - \left\| \frac{1 + \psi^{e,\star}}{\Delta\psi^e} L^e - \bar{L}^e \right\|_2 (1 + \max_i \|B_{:,i}^\star\|_2^2) \\ &\geq \frac{8^3(1 + \min_i \|B_{:,i}^\star\|_2^2)(1 + \psi^{e,\star})}{9^3(\max_k w_k^{e,\star})^2} \\ &\quad - \left\| \frac{1 + \psi^{e,\star}}{\Delta\psi^e} L^e - \bar{L}^e \right\|_2 (1 + \max_i \|B_{:,i}^\star\|_2^2) \end{aligned}$$

Where the last inequality follows from the relation (18). Thus, it suffices to show that:

$$\frac{8^3(1 + \min_i \|B_{:,i}^\star\|_2^2)(1 + \psi^{e,\star})}{9^3(\max_k w_k^{e,\star})^2} - \left\| \frac{1 + \psi^{e,\star}}{\Delta\psi^e} L^e - \bar{L}^e \right\|_2 (1 + \max_i \|B_{:,i}^\star\|_2^2) > 0. \quad (25)$$

To that end, we control the term $\left\| \frac{1+\psi^{e,*}}{\Delta\psi^e} L^e - \bar{L}^e \right\|_2$.

$$\begin{aligned}
& \left\| \frac{1+\psi^{e,*}}{\Delta\psi^e} L^e - \bar{L}^e \right\|_2 \\
& \leq 2 \left\| \underbrace{(M^e - \bar{M}^e)\Gamma^* \left[\frac{\Delta\psi^e}{1+\psi^{e,*}} \Gamma^{*T} M^e \Gamma^* + \frac{1}{1+\psi^{e,*}} \mathcal{I} \right]^{-1} \Gamma^{*T} M^e}_{\text{Term 1}} \right\|_2 \\
& \quad + \left\| \underbrace{(M^e - \bar{M}^e)\Gamma^* \left[\frac{\Delta\psi^e}{1+\psi^{e,*}} \Gamma^{*T} M^e \Gamma^* + \frac{1}{1+\psi^{e,*}} \mathcal{I} \right]^{-1} \Gamma^{*T} (M^e - \bar{M}^e)}_{\text{Term 2}} \right\|_2 \\
& \quad + \left\| \underbrace{\bar{M}^e \Gamma^* \left\{ \left[\frac{\Delta\psi^e}{1+\psi^{e,*}} \Gamma^{*T} M^e \Gamma^* + \frac{1}{1+\psi^{e,*}} \mathcal{I} \right]^{-1} - \left[\Gamma^{*T} \bar{M}^e \Gamma^* + \frac{1}{1+\psi^{e,*}} \mathcal{I} \right]^{-1} \right\} \Gamma^{*T} \bar{M}^e}_{\text{Term 3}} \right\|_2.
\end{aligned} \tag{26}$$

We bound each of the individual terms in (26). Using the inequalities $\left[\Gamma^{*T} M^e \Gamma^* + \frac{1}{\Delta\psi^e} \mathcal{I} \right]^{-1} \preceq (\Delta\psi^e) \mathcal{I}$ and $\|\tilde{M}^e\|_2 \leq \frac{1}{\min_k w_k^{e,*}}$ and the relation (22), Term 1 and Term 2 can be bounded as follows:

$$\begin{aligned}
\text{Term 1} & \leq \frac{10(1+C_\psi)^2 \|w^{1,*}\|_\infty \|\Gamma^*\|_2^2}{4(\min_k w_k^{e,*})^3} \\
\text{Term 2} & \leq \frac{25 \|\Gamma^*\|_2^4 (1+C_\psi)^3 \|w^{1,*}\|_\infty}{16(\min_k w_k^{e,*})^4}.
\end{aligned} \tag{27}$$

To bound Term 3, we use Taylor series expansion yielding

$$(A+E)^{-1} - A^{-1} = A^{-1} \sum_{k=1}^{\infty} (EA^{-1})^k.$$

Further, if $\|E\|_2 \|A^{-1}\|_2 < 1$, we can bound the spectral norm of the difference $(A+E)^{-1} - A^{-1}$ as follows:

$$\|(A+E)^{-1} - A^{-1}\|_2 \leq \|A^{-1}\|_2 \sum_{k=1}^{\infty} \|E\|_2^k \|A^{-1}\|_2^k = \frac{\|A^{-1}\|_2^2 \|E\|_2}{1 - \|E\|_2 \|A^{-1}\|_2} \tag{28}$$

In the context of Term 3, $E = \frac{\Delta\psi^e}{1+\psi^{e,*}} \Gamma^{*T} M^e \Gamma^* - \Gamma^{*T} \bar{M}^e \Gamma^*$ and $A = (1+\psi^{e,*}) \mathcal{I}$. One can check that $\|E\|_2 \leq \frac{(\frac{5}{4}C_\psi+1)\|\Gamma^*\|_2^2}{(\min_k w_k^{e,*})^2}$. Thus, employing the relation $(\min_k w_k^{e,*})^2 \geq 5(\frac{5}{4}C_\psi+1)\|\Gamma^*\|_2^2$, we have that:

$$\text{Term 3} \leq \frac{5\|\Gamma^*\|_2^4 (\frac{5}{4}C_\psi+1)}{4 \min_k (w_k^{e,*})^3} \tag{29}$$

Combining the bounds in (27) and (29) with (26), we find that:

$$\begin{aligned}
\left\| \frac{1+\psi^{e,*}}{\Delta\psi^e} L^e - \tilde{L}^e \right\|_2 & \leq \frac{10(1+C_\psi)^2 \|w^{1,*}\|_\infty \|\Gamma^*\|_2^2}{4(\min_k w_k^{e,*})^3} + \frac{25\|\Gamma^*\|_2^4 (1+C_\psi)^3 \|w^{1,*}\|_\infty}{16(\min_k w_k^{e,*})^4} \\
& \quad + \frac{5\|\Gamma^*\|_2^4 (\frac{5}{4}C_\psi+1)}{4 \min_k (w_k^{e,*})^3} \\
& \leq \left(\frac{10}{4} + \frac{25}{16} + \frac{5}{4} \right) \frac{(1+2C_\psi)^2 \max\{\|\Gamma^*\|_2^2, \|\Gamma^*\|_2^4\} \max\{1, \|w^{1,*}\|_\infty\}}{(\min_k w_k^{e,*})^3},
\end{aligned}$$

where the second inequality follows from $\min_k w_k^{e,*} \geq \|w^{1,*}\|_\infty (1+C_\psi)$. Thus, since $\frac{\min_k w_k^{e,*}}{\text{cond}(\text{diag}(w^{e,*}))} \geq 8\kappa^*(1+C_\psi)^2 \max\{\|\Gamma^*\|_2^2, \|\Gamma^*\|_2^4\} \max\{1, \|w^{1,*}\|_\infty\}$, the sufficient condition in (25) is satisfied. This concludes that if $\tilde{\psi}^e \neq \psi^{e,*}$ for $e \in \{2, 3\}$, $(\mathcal{I} - B^*)^T (M^e + L^e) (\mathcal{I} - B^*)$ will have a non-zero outside of the moral graph of B^*

and thus according to (21), $\text{moral}(B^*) \subset \text{moral}(\tilde{B})$. We have established the first component of Lemma 2. The second component (where $\psi^e = \psi^{e,*}$ for $e = 2, 3$) follows from (20).

We next provide a proof of Lemma 2 under Assumptions 1-5 in (11). Lemma 1 implies the following relations:

$$\begin{aligned}
& (\mathcal{I} - B^*)^{-1} \left(\text{diag} \left(w^{3,*} - (1 + \tilde{\psi}^3)w^{1,*} \right) + (\psi^{3,*} - \tilde{\psi}^3)\Gamma^*\Gamma^{*T} \right) (\mathcal{I} - B^*)^{-T} \\
&= (\mathcal{I} - \tilde{B})^{-1} \text{diag} \left(\tilde{w}^3 - (1 + \tilde{\psi}^3)\tilde{w}^1 \right) (\mathcal{I} - \tilde{B})^{-T} \\
& (\mathcal{I} - B^*)^{-1} \left(\text{diag} \left(w^{3,*} - \frac{1 + \tilde{\psi}^3}{1 + \tilde{\psi}^2} w^{2,*} \right) + \left(1 + \psi^{3,*} - (1 + \tilde{\psi}^3) \frac{1 + \psi^{2,*}}{1 + \tilde{\psi}^2} \right) \Gamma^*\Gamma^{*T} \right) (\mathcal{I} - B^*)^{-T} \quad (30) \\
&= (\mathcal{I} - \tilde{B})^{-1} \text{diag} \left(\tilde{w}^3 - \frac{(1 + \tilde{\psi}^3)}{1 + \tilde{\psi}^2} \tilde{w}^2 \right) (\mathcal{I} - \tilde{B})^{-T}
\end{aligned}$$

Using the relation (30) and a similar analysis as with the proof under Assumptions 1-5 in (10), one can arrive at the conclusion of Lemma 2 with Assumptions 1-5 in (11). \square

A.1.4 Proof of Lemma 3

Proof. We consider the setup with Assumptions 1-5 in (10) and for brevity, leave out the proof with Assumption 6-10 in (11). We have from (20) that for $e = 2, 3$:

$$\begin{aligned}
& (\mathcal{I} - B^*)^{-1} \text{diag} \left(w^{e,*} - (1 + \psi_e^*)w^{1,*} \right) (\mathcal{I} - B^*)^{-T} \\
&= (\mathcal{I} - \tilde{B})^{-1} \text{diag} \left(\tilde{w}^e - (1 + \psi_e^*)\tilde{d}^1 \right) (\mathcal{I} - \tilde{B})^{-T} \quad (31)
\end{aligned}$$

By Assumption 4 and 5, we have that $[w^{2,*} - (1 + \psi_e^*)w^{1,*}, w^{3,*} - (1 + \psi_e^*)w^{1,*}]$ has full row-rank and nonzero entries. From relation (31), we have:

$$\begin{aligned}
(\mathcal{I} - \tilde{B})(\mathcal{I} - B^*)^{-1} \text{diag} \left(w^{2,*} - (1 + \psi_e^*)w^{1,*} \right) (\mathcal{I} - B^*)^{-T} (\mathcal{I} - \tilde{B})^T &= \text{diag} \left(\tilde{w}^2 - (1 + \psi_e^*)\tilde{w}^1 \right) \\
(\mathcal{I} - \tilde{B})(\mathcal{I} - B^*)^{-1} \text{diag} \left(w^{3,*} - (1 + \psi_e^*)w^{1,*} \right) (\mathcal{I} - B^*)^{-T} (\mathcal{I} - \tilde{B})^T &= \text{diag} \left(\tilde{w}^3 - (1 + \psi_e^*)\tilde{w}^1 \right)
\end{aligned}$$

Let $\phi_k^e := \left[(\mathcal{I} - \tilde{B})(\mathcal{I} - B^*)^{-1} \text{diag} \left(w^{e,*} - w^{1,*}(1 + \psi_e^*) \right) \right]_k$, for any $k = 1, 2, \dots, p$. Let $\xi_k := \left[(\mathcal{I} - \tilde{B})(\mathcal{I} - B^*)^{-1} \right]_k$. Then for any $k = 1, 2, \dots, p$,

$$\phi_k^e \perp \xi_l \quad \text{for any } k \neq l \quad (32)$$

Notice that for any $k = 1, 2, \dots, p$, $\{\xi_l\}_{l \neq k}$ are linearly independent. The condition above means that ϕ_k^2 and ϕ_k^3 (where neither would be exactly a zero vector because $w^{2,*} - w^{1,*}(1 + \psi_e^*), w^{3,*} - w^{1,*}(1 + \psi_e^*) \neq 0$) live inside the one-dimensional null-space of the matrix formed by concatenating the vectors $\{\xi_l\}_{l \neq k}$. In particular, for every k , we have that for some constant $c \neq 0$: $\xi_k \text{diag} \left(w^{2,*} - w^{1,*}(1 + \psi_e^*) \right) = c \xi_k \text{diag} \left(w^{3,*} - w^{1,*}(1 + \psi_e^*) \right)$. It is straightforward to check the condition $\frac{w_k^{2,*} - (1 + \psi_e^*)w_k^{1,*}}{w_l^{2,*} - (1 + \psi_e^*)w_l^{1,*}} \neq \frac{w_k^{3,*} - (1 + \psi_e^*)w_k^{1,*}}{w_l^{3,*} - (1 + \psi_e^*)w_l^{1,*}}$ for $k, l \in S, k \neq l$ implies that:

$$\Xi_{m,:} = \begin{cases} \Xi_{m,S} = 0 \\ \Xi_{m,S} \text{ has one nonzero-component \& } \Xi_{m,S^c} = 0, \end{cases} \quad (33)$$

where $\Xi \in \mathbb{R}^{p \times p}$ be the matrix formed by concatenating the row vectors $\{\xi^i\}_{i=1}^p$ so that $\mathcal{I} - \tilde{B} = \Xi(\mathcal{I} - B^*)$. Since $\mathcal{I} - \tilde{B}$ and $\mathcal{I} - B^*$ are invertible, so must be Ξ .

The relation (33), that $S = \{1, 2, \dots, p\}$, and that Ξ is invertible implies that Ξ is a diagonal matrix up to row-permutations so that:

$$(\mathcal{I} - \tilde{B}) = \mathcal{K}_\pi D (\mathcal{I} - B^*),$$

where D is diagonal with all nonzero entries on the diagonal and $\tilde{\pi}$ is a permutation. We know that $(\mathcal{I} - \tilde{B})$ will have ones on the diagonal. Hence, it is straightforward to check that $\mathcal{K}_\pi = D = \xi(m)$ and thus $\tilde{B} = B^*$. \square

A.2 Role of \bar{h} in identifiability

In this section, we consider the role of \bar{h} (i.e. the number of latent variables in the model) for identifiability. Theorem 1 states that as long as Assumptions 1-5 in (10) or Assumptions 6-10 in (11) are satisfied, then identifiability is possible for any \bar{h} with $\bar{h} \geq h$. These assumptions rely on the exist of at least two interventional environments. In particular, we will first show that this is a necessary condition in the setting if $\bar{h} = p$. We will also show that if $\bar{h} = h$ and under some incoherence conditions (e.g. dense latent effects and sparse DAG structure), a single interventional environment is sufficient for identifiability.

A.2.1 $\bar{h} = p$

Suppose there is only a single interventional environment satisfying Assumptions 1-5, as an example. We will show that in addition to the population solutions, the MLE has an additional minimizer $\tilde{B}, \tilde{\Gamma}, \{(\tilde{w}^e, \tilde{\psi}^e)\}_{e=1}^m$ by showing that these parameters satisfy the requirement for an optimal solution in Lemma 1. We let $\psi^e = \psi^{e,*}$, \tilde{B} to be a connectivity matrix associated to a DAG in the Markov equivalence class of \mathcal{D}_X^* with $\tilde{B} \neq B^*$, and the parameters $\tilde{\Gamma}, \tilde{w}^1, \tilde{w}^2$ to be appropriately defined. Specifically, let \tilde{B} and $\tilde{w}^2 - \tilde{w}^1(1 + \tilde{\psi}^2)$ satisfy the following equations:

$$\begin{aligned} & (\mathcal{I} - B^*)^{-1}(\text{diag}(w^{2,*} - (1 + \psi^{2,*})w^{1,*}))(\mathcal{I} - B^*)^{-T} \\ &= (\mathcal{I} - \tilde{B})^{-1}(\text{diag}(\tilde{w}^2 - (1 + \tilde{\psi}^2)\tilde{w}^1))(\mathcal{I} - \tilde{B})^{-T}. \end{aligned} \quad (34)$$

In particular, we let \tilde{B} to be any Markov equivalent DAG to B^* and find \tilde{w}^1 such that $(\mathcal{I} - B^*)^{-1}\text{diag}(w^{1,*})(\mathcal{I} - B^*)^{-T} = (\mathcal{I} - \tilde{B})^{-1}\text{diag}(\tilde{w}^1)(\mathcal{I} - \tilde{B})^{-T}$ and \tilde{w}^2 such that $(\mathcal{I} - B^*)^{-1}\text{diag}(w^{2,*})(\mathcal{I} - B^*)^{-T} = (\mathcal{I} - \tilde{B})^{-1}\text{diag}(\tilde{w}^2)(\mathcal{I} - \tilde{B})^{-T}$. We then let $\tilde{w}^1 = \tilde{w}^1 - \mu$ and $\tilde{w}^2 = \tilde{w}^2 + (1 + \psi^{2,*})\mu$ for any non-negative vector μ . Thus, for this choice of parameters, (35) is satisfied. It remains to check that:

$$\begin{aligned} & (\mathcal{I} - B^*)^{-1}(\text{diag}(w^{1,*}) + \Gamma^*\Gamma^{*T})(\mathcal{I} - B^*)^{-T} \\ &= (\mathcal{I} - \tilde{B})^{-1}(\text{diag}(\tilde{w}^1) + \tilde{\Gamma}\tilde{\Gamma}^T)(\mathcal{I} - \tilde{B})^{-T}. \end{aligned}$$

Recalling that $\tilde{w}^1 = \tilde{w}^1 - \mu$, it is straightforward to find a full rank $\tilde{\Gamma}$ that satisfies the relation above.

A.2.2 $\bar{h} = h$

We consider the setting with a single interventional setting that satisfies Assumption 1-5 in (10). We show that under some incoherence-type assumptions, the *DirectLikelihood* procedure combined with choosing the sparsest moral graph has a unique optimum equaling B^* . By Lemma 2, we conclude that $\text{moral}(B^*) \subset \text{moral}(\tilde{B})$ unless $\tilde{\psi}^2 = \psi^{2,*}$. Since we are looking for the sparsest producing moral graph, we conclude that $\text{moral}(B^*) = \text{moral}(\tilde{B})$. By Lemma 1, we have that:

$$\begin{aligned} & (\mathcal{I} - B^*)^{-1}(\text{diag}(w^{e,*}) + (1 + \psi^{e,*})\Gamma^*\Gamma^{*T})(\mathcal{I} - B^*)^{-T} \\ &= (\mathcal{I} - \tilde{B})^{-1}(\text{diag}(\tilde{w}^e) + (1 + \tilde{\psi}^e)\tilde{\Gamma}\tilde{\Gamma}^T)(\mathcal{I} - \tilde{B})^{-T}. \end{aligned}$$

By the Woodbury inversion lemma, we have for both $e = 1, 2$:

$$\begin{aligned} & \left[(\mathcal{I} - B^*)^T \text{diag}(w^{e,*})^{-1}(\mathcal{I} - B^*) - (\mathcal{I} - \tilde{B})^T \text{diag}(\tilde{w}^e)^{-1}(\mathcal{I} - \tilde{B}) \right] + L^{e,*} \\ & \text{is rank } h, \end{aligned} \quad (36)$$

where $L^{e,*}$ is a rank h matrix with row and column space equal to the row and column space of $(\mathcal{I} - B^*)^T \text{diag}(w^{e,*})^{-1} \Gamma^*\Gamma^{*T} \text{diag}(w^{e,*})^{-1}(\mathcal{I} - B^*)^T$. Notice that the quantity inside the brackets in (36) lies inside the moral graph of B^* . We now use rank-sparsity incoherence [4] to conclude that the term inside the bracket in (36) vanishes. In particular, if the tangent space of the sparse variety at the moral graph of B^* is transverse with the tangent space of the low rank variety at $L^{e,*}$, then (36) is satisfied if and only if for $e = 1, 2$

$$\left[(\mathcal{I} - B^*)^T \text{diag}(w^{e,*})^{-1}(\mathcal{I} - B^*) - (\mathcal{I} - \tilde{B})^T \text{diag}(\tilde{w}^e)^{-1}(\mathcal{I} - \tilde{B}) \right] = 0. \quad (37)$$

The transversality of the tangent spaces is satisfied if the latent effects are dense and \mathcal{D}_X^* is sparse. Thus, following the same strategy as the proof of Lemma 3, we conclude from the relations (37) that $\tilde{B} = B^*$.

A.3 Single parameter perturbation setting

As discussed in Section 2.1, one may fit to data the perturbation model (2) where the perturbation magnitudes are equal in magnitude across the coordinates, e.g. $\text{var}(\delta^e) = \zeta_e^* \mathbf{1}$ for the parameter vector $\zeta^* \in \mathbb{R}^m$. Fitting such a model can be achieved by the reparametrization $v^e = v + \zeta^e \mathbf{1}$ of the decision variable w^e in (5) for parameter vectors $v \in \mathbb{R}^p$ and $\zeta \in \mathbb{R}^m$. We assume an observational environment $e = 1$ and two interventional environments $e = 2, 3$ and modify Assumption 3 and 5 appropriately in this setting as follows:

Modified Assumption 3 – heterogeneity among the perturbations:

$$\text{the vectors } \begin{pmatrix} \psi^{2,*} \\ \psi^{3,*} \end{pmatrix} \text{ \& } \begin{pmatrix} \zeta^{2,*} \\ \zeta^{3,*} \end{pmatrix} \text{ are linearly independent.} \quad (38)$$

Modified Assumption 5 – perturbation is sufficiently strong for $e = 3$

$$\zeta_3^* \geq 8\kappa^*(1 + 2C_\psi)^2(1 + \|v^{2,*}\|_\infty)(1 + \|\Gamma^*\|_2^2 + \|\Gamma^*\|_2^4)$$

With this modification, we have the following consistency guarantees:

Theorem 5 (Single parameter perturbation with perturbed hidden variables). *Suppose Assumption 1,2,4 in (11) and Assumption 3 and 5 in (38) are satisfied. The following assertions hold:*

1. $B^* \in B_{opt}$ and any other optimum $B \in B_{opt}$ satisfies: $\text{moral}(B^*) \subseteq \text{moral}(B)$.
2. The optimum of $\arg \min_{B \in B_{opt}} \|\text{moral}(B)\|_{\ell_0}$ is unique and equal to B^* .

We next provide identifiability guarantees in the setting without hidden perturbations (i.e. $\psi^{e,*} = 0$ for all e) with single parameter perturbation. Fitting such a model can be achieved by the reparametrization $w^e = w + \zeta^e \mathbf{1}$ for a parameter vector $\zeta^e \in \mathbb{R}_+$ and $\psi^e \equiv 0$. We then have the following identifiability in this setting.

Theorem 6 (Single parameter perturbation with unperturbed hidden variables). *Suppose Assumption 1 and 2 in (10) are satisfied for only environments $e = 2$. Then, if $\zeta^{2,*} > 0$, $\mathcal{D}_{opt} = \mathcal{D}_X^*$ and $B_{opt} = B^*$.*

A.3.1 Proof of Theorem 5

Proof. The proof of the first part closely mirrors that of Theorem 1 and is left out for brevity. It concludes that $\tilde{\psi}^e = \psi^{e,*}$ for $e = 1, 2, 3$. To prove the second part, suppose that in addition to the population parameters $(B^*, \Gamma^*, \{(\psi^{e,*}, \zeta^{e,*})\}_{e=1}^m)$, *DirectLikelihood* has another solution $(\tilde{B}, \{(\tilde{\psi}^e, \tilde{\zeta}^e)\}_{e=1}^m)$. Then, since the first environment does not consist of any perturbations, we find that:

$$\begin{aligned} \Sigma^{2,*} - \Sigma^{1,*} &= (\mathcal{I} - B^*)^{-1}(\zeta^{2,*}\mathcal{I} + \psi^{2,*}\Gamma^*\Gamma^{*T})(\mathcal{I} - B^*)^{-T} \\ &= (\mathcal{I} - \tilde{B})^{-1}(\tilde{\zeta}^2\mathcal{I} + \psi^{2,*}\tilde{\Gamma}\tilde{\Gamma}^T)(\mathcal{I} - \tilde{B})^{-T} \\ \Sigma^{3,*} - \Sigma^{1,*} &= (\mathcal{I} - B^*)^{-1}(\zeta^{3,*}\mathcal{I} + \psi^{3,*}\Gamma^*\Gamma^{*T})(\mathcal{I} - B^*)^{-T} \\ &= (\mathcal{I} - \tilde{B})^{-1}(\tilde{\zeta}^3\mathcal{I} + \psi^{3,*}\tilde{\Gamma}\tilde{\Gamma}^T)(\mathcal{I} - \tilde{B})^{-T} \end{aligned}$$

Due to Assumption 3, there exists $a \in \mathbb{R}^2$ such that $a^T \begin{pmatrix} \psi^{2,*} \\ \psi^{3,*} \end{pmatrix} = 0$ but $a^T \begin{pmatrix} \zeta^{2,*} \\ \zeta^{3,*} \end{pmatrix} \neq 0$. Then,

$$\begin{aligned} a_1(\Sigma^{2,*} - \Sigma^{1,*}) + a_2(\Sigma^{3,*} - \Sigma^{1,*}) &= a^T \begin{pmatrix} \zeta^{2,*} \\ \zeta^{3,*} \end{pmatrix} (\mathcal{I} - B^*)^{-1}(\mathcal{I} - B^*)^{-T} \\ &= a^T \begin{pmatrix} \tilde{\zeta}^2 \\ \tilde{\zeta}^3 \end{pmatrix} (\mathcal{I} - \tilde{B})^{-1}(\mathcal{I} - \tilde{B})^{-T} \end{aligned}$$

Lastly, by appealing to identifiability of DAG under equal variances [22], we have that $\tilde{B} = B^*$. We further note that asymptotic convergence results similar to Corollary 1 may be shown but is left out for brevity. \square

A.3.2 Proof of Theorem 6

Proof. We will show in Lemma 4 that for $e = 1, 2$:

$$\begin{aligned}\Sigma^{e,*} &= (\mathcal{I} - B^*)^{-1} \left(\text{diag}(w^{1,*} + \zeta^{e,*}\mathbf{1}) + \Gamma^* \Gamma^{*T} \right) (\mathcal{I} - B^*)^{-T} \\ &= (\mathcal{I} - \tilde{B})^{-1} \left(\text{diag}(\tilde{w}^1 + \tilde{\zeta}^e \mathbf{1}) + \tilde{\Gamma} \tilde{\Gamma}^T \right) (\mathcal{I} - \tilde{B})^{-T}\end{aligned}\quad (39)$$

Taking the difference $\Sigma^{2,*} - \Sigma^{1,*}$, the relation (39) yields:

$$\begin{aligned}\Sigma^{2,*} - \Sigma^{1,*} &= \zeta^{2,*} (\mathcal{I} - B^*)^{-1} (\mathcal{I} - B^*)^{-T} \\ &= \tilde{\zeta}^2 (\mathcal{I} - \tilde{B})^{-1} (\mathcal{I} - \tilde{B})^{-T}.\end{aligned}\quad (40)$$

We can then appeal to identifiability of DAGs with equal noise variance [22] to conclude that $\tilde{B} = B^*$. \square

A.4 Proof of Theorem 2 and Theorem 3

We consider the proof of the case with unperturbed hidden confounders and leave out the proof for the setting without hidden confounders. For notational convenience, we state the extended population *DirectLikelihood* estimator (5) in the setting with unperturbed hidden variables as:

$$\begin{aligned}\arg \min_{\substack{B \in \mathbb{R}^{p \times p}, \Gamma \in \mathbb{R}^{p \times \bar{h}} \\ \{w^e\}_{e=1}^m \subseteq \mathbb{R}_{++}^p}} \sum_{e=1}^m \pi^{e,*} \ell^e(B, \Gamma, w^e; \Sigma^{e,*}, \text{do}(e)) \\ \text{subject-to } B \text{ DAG}\end{aligned}\quad (41)$$

where,

$$\begin{aligned}\ell^e(B, \Gamma, w^e; \Sigma^{e,*}, \text{do}(e)) &= \log \det (\text{diag}(w^e) + [\Gamma \Gamma^T]_{\text{do}(e)^c}) \\ &\quad + \text{trace} \left((\text{diag}(w^e) + [\Gamma \Gamma^T]_{\text{do}(e)^c})^{-1} (\mathcal{I} - \mathcal{F}_{\text{do}(e)^c} B) \Sigma^{e,*} (\mathcal{I} - \mathcal{F}_{\text{do}(e)^c} B)^T \right).\end{aligned}$$

As with Lemma 1, we characterize the optimal solutions of (41) in the following lemma.

Lemma 4. *Optimal solutions of (41) satisfy the following equivalence*

$$\begin{aligned}(B, \Gamma, \{w^e\}_{e=1}^m) \text{ optimum to (41)} \\ \iff \\ B \text{ DAG, } \{w^e\}_{e=1}^m \in \mathbb{R}_{++}^p, \Gamma \in \mathbb{R}^{p \times \bar{h}} \text{ with } \bar{h} \geq h \text{ and} \\ \Sigma^{e,*} = (\mathcal{I} - \mathcal{F}_{\text{do}(e)^c} B)^{-1} (\text{diag}(w^e) + [\Gamma \Gamma^T]_{\text{do}(e)^c}) (\mathcal{I} - \mathcal{F}_{\text{do}(e)^c} B)^{-T} \text{ for } e = 1, 2, \dots, m\end{aligned}$$

The proof of Lemma 4 is similar to Lemma 1 and left out for brevity. Based on the result of Lemma 4, any optimum $(B, \Gamma, \{w^e\}_{e=1}^m)$ of population *DirectLikelihood* must satisfy the relation for each $e = 1, 2, \dots, m$.

$$\Sigma^{e,*} = (\mathcal{I} - \mathcal{F}_{\text{do}(e)^c} B)^{-1} ([\Gamma \Gamma^T]_{\text{do}(e)^c} + \text{diag}(w^e)) (\mathcal{I} - \mathcal{F}_{\text{do}(e)^c} B)^{-T} \text{ for } e = 1, 2, \dots, m \quad (42)$$

Aside from $(B^*, \{w^{e,*}\}_{e=1}^m)$, suppose there is another solution $(\tilde{B}, \{\tilde{w}^e\}_{e=1}^m)$ satisfying (42). Thus, we have for $e = 2, 3$:

$$\begin{aligned}\Sigma^{e,*} - \Sigma^{1,*} &= (\mathcal{I} - B^*)^{-1} \text{diag}(w^{e,*} - w^{1,*}) (\mathcal{I} - B^*)^{-T} \\ &= (\mathcal{I} - \tilde{B})^{-1} \text{diag}(\tilde{w}^e - \tilde{w}^1) (\mathcal{I} - \tilde{B})^{-T}\end{aligned}\quad (43)$$

Equation (43) yields the relation for $e = 2, 3$:

$$(\mathcal{I} - \tilde{B})(\mathcal{I} - B^*)^{-1} \text{diag}(w^{e,*} - w^{1,*}) (\mathcal{I} - B^*)^{-T} (\mathcal{I} - \tilde{B})^T = \text{diag}(\tilde{w}^e - \tilde{w}^1).$$

Let $\phi_k^e := [(\mathcal{I} - \tilde{B})(\mathcal{I} - B^*)^{-1} \text{diag}(w^{e,*} - w^{1,*})]_{k,:}$ for any $k = 1, 2, \dots, p$. Let $\xi_k := [(\mathcal{I} - \tilde{B})(\mathcal{I} - B^*)^{-1}]_{k,:}$. Then for any $k = 1, 2, \dots, p$, Then for any $k = 1, 2, \dots, p$,

$$\phi_k^e \perp \xi_l \text{ for any } k \neq l \quad (44)$$

Notice that for any $k = 1, 2, \dots, p$, $\{\xi_l\}_{l \neq k}$ are linearly independent. The condition above means that ϕ_k^2 and ϕ_k^3 (where neither would be exactly a zero vector because $w^{2,*} - w^{1,*}, w^{3,*} - w^{1,*} \neq 0$) live inside the one-dimensional null-space of the matrix formed by concatenating the vectors $\{\xi_l\}_{l \neq k}$. As with the proof of part 2 of Theorem 1, the assumption that $\frac{w_k^{2,*} - w_k^{1,*}}{w_l^{2,*} - w_l^{1,*}} \neq \frac{w_k^{3,*} - w_k^{1,*}}{w_l^{3,*} - w_l^{1,*}}$ for $k, l \in S, k \neq l$ implies that the matrix Ξ consisting of concatenating the row vectors $\{\xi^i\}_{i=1}^p$ satisfies relation (33).

Proof of part (a): The relation (33) and that Ξ is invertible implies that Ξ is a diagonal matrix up to row-permutations so that:

$$(\mathcal{I} - \tilde{B}) = \mathcal{K}_\pi D (\mathcal{I} - B^*),$$

where D is diagonal with all nonzero entries on the diagonal and $\tilde{\pi}$ is a permutation. We know that $(\mathcal{I} - \tilde{B})$ will have ones on the diagonal. Hence, it is straightforward to check that $\mathcal{K}_\pi = D = \xi(m)$ and thus $\tilde{B} = B^*$.

Proof of part (b): Suppose B^* and \tilde{B} and Ξ are ordered according to ancestors of X_p , then X_p and then the remaining variables. Since the underlying graph is a DAG, there is an ancestor of X_p that does not have any parent. We first consider this variable. Suppose $\Xi_{1,:}(S) = 0$. Then, since $\Xi_{1,:}$ is zero on this variable and its children, then $\Xi_{1,:}[(\mathcal{I} - B^*)_{:,1}]$ will be zero. This is a contradiction since $(\mathcal{I} - \tilde{B})$ has diagonal elements equal to one. By condition (33) and that $(\mathcal{I} - \tilde{B})$ must be diagonal, then $\Xi_{1,:}$ must have one nonzero entry, on either this ancestor variable or its children. Suppose for purposes of contradiction that this nonzero value happened on one of the children. Notice that if $\Xi_{j,1}$ is nonzero for some $j \neq 1$, then condition (33) implies that $\Xi_{j,:} = c_1 e_1$ for some constant c_1 . However, since the variable corresponding to index j is not a parent to the variable corresponding to index 1, then $\Xi_{j,:}(\mathcal{I} - B^*)_{:,j}$ will be zero. With this logic, $\Xi_{j,1}$ will have all zeros, leading to a contradiction since Ξ must be invertible. Hence, $\Xi_{1,:}$ must be of the form $\Xi_{1,:} = c_2 e_1$ for some constant c_2 . Since the diagonal elements of $\mathcal{I} - \tilde{B}$ are exactly one, then $c_2 = 1$. Repeating the same argument, and letting \bar{S} denote the set of variables X_p and the ancestors of X_p , we find that $\Xi_{\bar{S},:} = (\mathcal{I}_{|\bar{S}|} \quad 0_{|\bar{S}^c|})$. Hence we have that $\tilde{B}_{k,:} = B_{k,:}^*$ for all k corresponding to target variable X_p and all ancestors of X_p . Now suppose that S includes X_p and descendants of X_p . Let \hat{B}, B^*, Ξ be organized in descending order the descendants of X_p , X_p and then everything else. Since the underlying graph is a DAG, there is one or more descendants of X_p that do not have any children. Let \bar{S} be this collection. Since $\Xi_{\bar{S},:}(\mathcal{I} - B^*)_{:, \bar{S}}$ must have diagonal equal one, and because of the condition (33), then $\Xi_{\bar{S}, \bar{S}} = \mathcal{I}_{|\bar{S}|}$. Now consider any parent of these nodes that is a descendant of X_p . Since $\Xi_{|\bar{S}|+1,:}(\mathcal{I} - B^*)_{:, |\bar{S}|+1}$ must equal one and (33), then $\Xi_{|\bar{S}|+1,:}$ must have only one nonzero entry on S , either entries corresponding to its descendants or the variable itself. If this non-zero is in the location of one of the descendants, then Ξ will have two identical rows, meaning that it would not be invertible. This reasoning can be repeated until we arrive at the index corresponding to X_p and show that $\Xi_{p,:} = e_p$. Hence, $\tilde{B}_{p,:} = B_{p,:}^*$.

Proof of part (c): We prove that when the target variable and its parents all receive shift interventions and the DAG B^* is faithful with respect to underlying distribution, the sparsest optimum \tilde{B} satisfies $\tilde{B}_{p,:} = B_{p,:}^*$. Any of the sparsest optimum DAGs with same v-structures and skeletons as the population DAG. From the discussion above, Ξ will satisfy the relation (33) where S denotes the set of variables that have received a shift intervention. Suppose for the sake of contradiction that $\Xi_{p,:} \neq e_p$ (e.g. the estimated causal parents are not equal to the true causal parents). Since Ξ is invertible, the property (33) and that $\Xi(\mathcal{I} - B^*)$ must have nonzero diagonal elements, it must be that for one of the parents of X_p , denoted by index t , $\Xi_{t,:} = e_p$. With respect to the graph, this means that we are considering a graph where the edge between the parent of X_p and X_p is reversed. This edge reversal of course can be continued along the path of the descendants of X_p as long as this descendant has only a single parent. Suppose at any one of the descendants, the edge reversal stops so that this descendant becomes a source node. Let s be the index of this variable. Consider a node $s' \neq s$ that is not a parent or ancestor of X_p . Starting from the last descendant of this node, denoted by index s'_l , $\Gamma_{s,s'_l} = 0$ since otherwise this would imply that s'_l is a parent to s , contradicting that s is a source node. Working upwards from this last descendant, we can see that $\Gamma_{s,s'} = 0$. Furthermore, for any parent of X_p denoted by k , $\Gamma_{s,k} = 0$ since otherwise based on condition (33), $\Gamma_{s,k} = c e_k$, which would mean that the node k is a parent to s , contradicting that s is a source node. Following this logic upwards, we can also conclude that $\Gamma_{s,k} = 0$ for k being an ancestor of X_p . Since Γ is invertible, it remains that $\Gamma_{s,s} \neq 0$. This again leads to a contradiction to s being a source node since it would mean that s in the estimated DAG would have the same parents as the population DAG, and this set of parents is non-empty since s is a descendant of X_p . These contradictions would imply that $\Xi_{p,:} = e_p$.

A.5 Proof of Theorem 4

Proof. For any connectivity matrix B , latent coefficient Γ , noise variance w^1 :

$$\text{KL}(\Sigma^{e,\star}, \hat{\Sigma}_{B,\Gamma,w^1}(\bar{\zeta}^e, \bar{\psi}^e)) \geq \text{KL}(\Sigma^{e,\star}, \hat{\Sigma}_{B^\star,\Gamma^\star,w^{1,\star}}(\bar{\zeta}^e, \bar{\psi}^e)) = 0.$$

Thus, if there exists optimum $(\tilde{B}, \tilde{\Gamma}, \tilde{w}^1)$ to the max-risk optimization problem (14), it must satisfy for all $\mathcal{P}_e \in \mathcal{P}_{C_\zeta, C_\psi}$ the relation $\Sigma^{e,\star} = \hat{\Sigma}_{\tilde{B}, \tilde{\Gamma}, \tilde{w}^1}(\bar{\zeta}^e, \bar{\psi}^e)$. We take three environments: first one corresponding to the observational setting $e = 1$ where none of the variables are intervened on, a second environment $e = 2$ corresponding to setting where only the hidden variables are perturbed, and a last environment $e = 3$ that satisfies the assumptions of Theorem 4. We then appeal to Theorem 5 to conclude the desired result. □